Evaluation of system strength in a converter-dominated power system

EENX30

Master's thesis in Sustainable electric power engineering and electromobility

Malte Rosengren

DEPARTMENT OF ELECTRICAL ENGINEERING

CHALMERS UNIVERSITY OF TECHNOLOGY
Gothenburg, Sweden 2025
www.chalmers.se

Master's thesis 2025

Evaluation of system strength in a converter dominated power system

Malte Rosengren

CHALMERS
UNIVERSITY OF TECHNOLOGY

Department of Electrical Engineering
Division of Electric Power Engineering
Chalmers University of Technology
Gothenburg, Sweden 2025

Evaluation of system strength in a converter dominated power system
Malte Rosengren

Supervisors:
Ehsan Behrouzian, Svenska kraftnät
Fabian Hohn, Svenska Kraftnät
Examiner:
Massimo Bongiorno, Division of Electric Power Engineering

Master's Thesis 2025
Department of Electrical Engineering
Division of Electric Power Engineering

Chalmers University of Technology
SE-412 96 Gothenburg
Telephone +46 31 772 1000

Typeset in LaTeX
Gothenburg, Sweden 2025

Abstract

The steady increase in power electronic-interfaced generation, driven by the continued growth of renewable energy sources, is altering the dynamic behavior of modern power systems. While traditional system dynamics have been dictated by the characteristics of synchronous generators, the increasing penetration of Converter-Based Resources (CBRs) is contributing to a gradual transition toward converter-dominated power systems. This transition introduces new challenges to power system stability and raises questions regarding the applicability of conventional system strength metrics, particularly the Short Circuit Ratio (SCR), which has historically been used to assessgrid strength.

The aim of this thesis is to evaluate the limitations of the SCR metric in grid strength assessment for converter-dominated power systems and to assess alternative system strength metrics that may be more suitable under these changing conditions. Furthermore, the alternative system strength metrics need to be applicable during grid planning and is therefore restricted to the data available at this stage. The study was structured into three phases: (1) an initial review of the traditional grid strength metric, SCR, supported by Electromagnetic Transient (EMT) simulations; (2) initial evaluation and selection of alternative system strength metrics through comparative evaluation using small-scale case study with EMT simulations; and (3) implementation and evaluation in PSS®E, of the most promising metrics selected in (2), followed by validation of PSS®E results through detailed EMT simulations to determine the most reliable metric for system strength assessment.

The results indicate that traditional SCR metric consistently overestimates system strength in systems with high CBR penetration. The preliminary grid strength asessment conducted in phase 2 identified the Available Fault Level (AFL), Equivalent Short Circuit Ratio (EqSCR), and Site-Dependent Short Circuit Ratio (SDSCR) as the most appropriate alternative metrics for evaluating grid strength. While the AFL demonstrated promise in the initial small-scale review, it exhibited inconsistencies in the estimation of system strengthduring the validation process in phase 3. The results obtained from the EqSCR and SDSCR metrics were closely aligned. This outcome is expected, as both methods are fundamentally similar, differing primarily in the specific computational approaches they employ. For both small-scale (phase 2) and more complex system models (phase 3), the two metrics consistently identified the point of instability. System weakness and instability were observed at EqSCR values ranging from 1.1 to 1.3, and SDSCR values between 1.2 and 1.4. Given their comparable performance, EqSCR was identified as the more suitable metric due to its greater computational efficiency. Based on these findings, this thesis recommends the use of EqSCR for system strength screening in converter-dominated power systems.

Keywords: Power system stability, System strength, CBR, SCR, AFL, EqSCR, SDSCR

Acknowledgements

First and foremost, I would like to express my gratitude to my two supervisors at Svenska kraftnät, Ehsan Behrouzian and Fabian Hohn, for their time, dedication, and support throughout this work. Their guidance and expertise have been instrumental, and this thesis would not have been possible without their contributions.

I would also like to extend my appreciation to all the colleagues in my unit at Svenska kraftnät, whose genuine interest in the project small tips and feedback have greatly supported me along the way.

Additionally, I would like to express my gratitude to Professor Massimo Bongiorno at Chalmers University of Technology, who served as my examiner and provided valuable oversight to ensure I remained on track throughout the project.

Lastly, I would like to thank my family and friends for their unwavering support throughout these five years of study at Chalmers. Their encouragement has been a constant source of strength and motivation.

Malte Rosengren, Gothenburg, June 2025

List of Acronyms

AC	Alternating Current
AEMO	Australian Energy Market Operator
AFL	Available Fault Level
CBR	Converter-Based Resource
CMIIF	Classical Multi-Infeed Interaction Factor
CSCR	Composite Short Circuit Ratio
DC	Direct Current
DFT	Discrete Fourier Transform
DFIG	Doubly-Fed Induction Generator
EMIIF	Extended Multi-Infeed Interaction Factor
EMT	Electromagnetic Transient
EqSCR	Equivalent Short Circuit Ratio
ERCOT	Electric Reliability Council of Texas
ESCR	Effective Short Circuit Ratio
GFL	Grid-Following
GFM	Grid-Forming
HVDC	High Voltage Direct Current
IF	Interaction Factor
IILSCR	Inverter Interaction Level Short Circuit Ratio
ISCR	Interactive Short Circuit Ratio
LCC	Line-Commutated Converter
MIESCR	Multi-Infeed Effective Short Circuit Ratio
MIIF	Multi-Infeed Interaction Factor
NRSCR	Network Response Short Circuit Ratio
OH-line	Overhead Line
PLL	Phase-Locked Loop
POC	Point of Connection
RF	Radiality Factor
RMS	Root Mean Square
SCR	Short Circuit Ratio
SCRIF	Short Circuit Ratio with Interaction Factor
SDSCR	Site-Dependent Short Circuit Ratio
SLD	Single-Line Diagram
SG	Synchronous Generator
SSCI	Sub-Synchronous Control Interaction
SSR	Sub-Synchronous Resonance
SSTI	Sub-Synchronous Torsional Interaction
SVC	Static Var Compensator
SVK	Svenska Kraftnät
TSO	Transmission System Operator
UIF	Unit Interaction Factor
VSC	Voltage Source Converter
WSCR	Weighted Short Circuit Ratio

Contents

1
Introduction

Since the 1980s, climate change has become a growing concern. While initial actions were slow, the 2015 signing of the Paris Agreement by more than 190 countries and parties marked a major milestone [1]. With this agreement, a large majority of the world committed to limiting the rise in global temperature to 1.5 °C by reducing carbon dioxide emissions by 45 % by 2030 and achieving net-zero emissions by 2050 [1]. An essential part of achieving these goals is the electrification of society and the transition to renewable energy sources. The impact of this is evident in the rapid expansion of wind and solar power, which increased from approximately 4.4 % of global electricity generation in 2013 to 13 % in 2023 [2]. A similar development has occurred in Sweden, where the installed capacity of wind and solar power grew significantly, from 6.4 GW and 0.15 GW, respectively, in 2016 to 16.2 GW and 3.97 GW in 2023 [3].

Both wind and solar generation depend on power electronic converters to interface with the AC grid. For solar photovoltaic (PV) systems, DC/AC inverters convert the generated DC power into AC [4]. In wind energy, power electronics enable variable-speed operation, improving energy capture and system efficiency. The increasing adoption of Type 4 wind turbines, which use full converter systems (AC/DC–DC/AC), demonstrates this shift, allowing the generator to be decoupled from the grid, thus enabeling synchronization and enhanced control over active and reactive power output [4], [5].

The evolution of power systems from synchronous to converter-based generation began with the deployment of High Voltage Direct Current (HVDC) links and has accelerated with the large-scale integration of wind and solar energy. In Sweden, the increasing dominance of converter-based resources (CBRs) introduces new challenges to maintaining system stability, such as frequency regulation, voltage support, dynamic response, and the risk of control interactions [6]. Moreover, the shift toward converter-based technologies extends beyond generation alone. Battery energy storage systems are seeing steady growth, while the green industrial transition in northern Sweden is introducing significant power electronic loads, such as hydrogen electrolyzers [7]. Addressing the challenges posed by this transition requires the development of new control strategies and grid-support technologies to ensure stable and reliable operation in future power systems dominated by renewable and converter-interfaced generation.

1.1 Problem Description

The connection of new CBRs to the power system requires thorough planning to ensure the maintenance of stable operation. Screening methods play an integral role in the early stages of this process, offering estimates of system strength and stability by identifying potential risks under a wide range of system conditions [8]. Given the variety of possible operating conditions, emphasis is placed on speed through reduced complexity, though this comes at the cost of reduced accuracy. Despite this limitation in accuracy, the advantage is a reduction in overall resources required. This is because resource-intensive and detailed investigations can be focused on cases highlighted by the screening metric.

The most widely used screening metric in planning the connections of CBRs is the Short Circuit Ratio (SCR). This metric has traditionally been employed to assess system strength when integrating various plant types, including Synchronous Generators (SGs), HVDC systems, and more recently, CBRs [8]. It is based on the assumption that the planned plant is connected to an infinite bus, with the power system represented by a Thévenin impedance model. However, the shift toward a converter-dominated power system introduces the risk of interactions between multiple CBRs, which could negatively affect power system stability.

The Swedish Transmission System Operator (TSO), Svenska Kraftnät (SVK), has identified the need to evaluate traditional system strength metrics used in their screening of new CBR connections. They recognize the necessity to explore alternative screening metrics which more effectively account for interactions between CBRs and their potential impact on power system stability.

1.2 Aim

This thesis aims to examine the limitations of the traditional system strength metric in a converter-dominated power system and to assess potential alternative screening metrics that are more suitable to future power system conditions. Additionally, the thesis seeks to investigate how the thresholds of such a replacement metric should be defined to distinguish weak and strong points in the system. The outcome should be a screening method that, at an early stage of planning, can identify vulnerable areas for integrating CBRs into a grid with a high penetration of such resources.

1.3 Research Questions

Given the aim of the thesis the following research questions were formulated.

- What are the limitations of SCR in a converter dominated power system?
- How can system strength be redefined and evaluated in systems with high penetration of CBRs?

- What thresholds should be defined to ensure stable operation when using alternative metrics for estimating system strength?

1.4 Scope

This thesis focuses on evaluating system strength in the context of small-signal stability within converter-dominated power systems. The emphasis is placed on identifying and assessing screening metrics capable of capturing the dynamic interactions between CBRs and evaluating the effects these interactions have on system strength. Aspects of power system stability related to large-signal disturbances, such as Fault Ride Through (FRT) performance, are not addressed in this work, since they are considered beyond the scope of this thesis.

When evaluating alternative screening metrics for system strength the following constraints were considered.

- The metric must be applicable using the limited data typically available during the early stages of power grid planning.
- The metric should account for the interactions between multiple CBRs within the grid.
- The metric should not utilize Electromagnetic Transient (EMT) simulations.

The EMT-based simulation studies conducted in this work are intended to verify the alternative metrics and are focused exclusively on Type 3 and Type 4 wind farms as representations of CBRs; other types of converter-based generation—such as solar PV, HVDC systems, and battery energy storage—were not considered. Similarly, large scale power electronic loads, including emerging applications such as hydrogen production via electrolyzers and high-demand data centers, were not considered.

These delimitations were necessary to constrain the scope of the thesis to a manageable and feasible extent. The decision to focus on Type 3 and Type 4 wind turbines was based on their significant growth and established presence in power systems over the past decade. Although there are ongoing developments and future plans for large-scale power electronic loads, as well as for battery energy storage systems, these technologies have not yet reached the same level of penetration or remain projections for the future.

1.5 Outline

This section provides an outline of the overall structure of this master's thesis. Figure 1.1 illustrates this structure, in which the first chapter presents an introduction to the thesis, including a problem description as well as an overview of the overall aim and scope of the work.

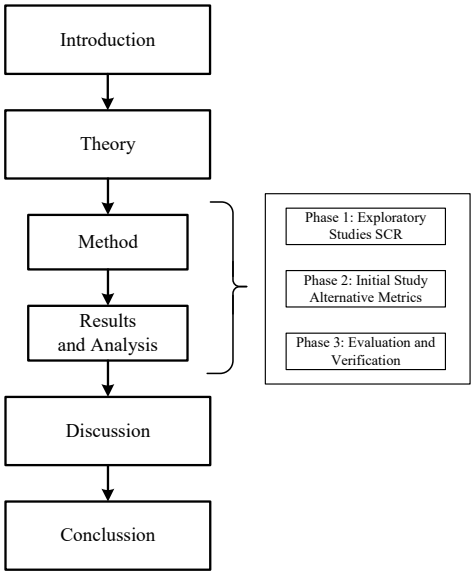

Figure 1.1: Outline of the report

The second chapter presents the theoretical background necessary to provide the reader with the required context. This chapter introduces both traditional and emerging power system stability concepts, explains the core principles of traditional system strength, and described the different screening metrics available for estimating system strength in a converter-dominated power system.

The third and fourth chapters present the methodology and results of the thesis. These chapters include three phases; the initial evaluation of traditional system strength (phase 1), the initial evaluation of alternative system strength metrics through small-scale case studies with selection of the most promising alternative system strength metrics (phase 2) and the final detailed evaluation validation of the most promising alternative system strength metrics conducted in PSS®E with verification through EMT simulations in PSCAD (phase 3).

The fifth chapter discusses the key findings of the thesis, addresses its limitations, proposes directions for future work, and considered ethical considerations related to the screening of system strength and the integration of converter-based resources. The final chapter addresses the research questions of the thesis and presents the conclusions of this master's thesis.

2
Theory

This chapter presents the theoretical foundations relevant to this thesis. It begins by explaining how power electronic converters are used in power generation, followed by an overview of the fundamental concepts of power system stability and system strength. Finally, it introduces a selection of metrics that may be used to assess system strength, particularly in converter-dominated power systems.

2.1 Converter Interfaced Power Generation

While the power system requires an AC voltage with a stable nominal frequency, renewable energy sources such as solar, primarily PV generation, and wind can be intermittent or generate DC power. To interface with the power system, power electronic converters are necessary to regulate voltage, frequency, and power output [4]. This is typically achieved through DC/AC inverters, AC/DC rectifiers, or DC/DC converters. These technologies enable the connection of DC-generating PVs to the AC grid and allow wind turbines, which are subject to varying wind speeds, to maintain a stable output frequency. Due to the focus on the simulation of Type 3 and Type 4 wind farms in this project this section will only cover these two types of CBRs. However, it is important to note that there are other types of CBRs in the power system such as PV generation, HVDC and battery energy storage which rely on power electronic converters as well.

2.1.1 Type 3 Wind Turbine

The Type 3 wind turbine is usually referred to as a Doubly-Fed Induction Generator (DFIG) turbine. This designation indicates that the stators is directly connected to the grid, while the rotor circuit is connected to the grid via the back-to-back converter system, as illustrated in the overview of the Type 3 turbine components in Figure 2.1.

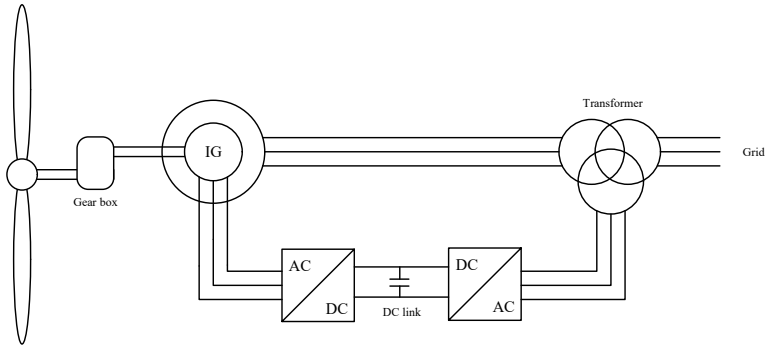

Figure 2.1: Overview key components Type 3 wind turbine

The converter allows for the extraction of energy from the rotor winding, which was not possible with previous generations of wind turbines [4]. Additionally, the converter allows for control of rotor current and frequency [9], [10]. Therefore, the DFIG turbine is able to provide power at both super-synchronous and sub-synchronous rotor speeds, which allows for a much larger operating range for the turbine. Another advantage of the converter is the level of control it allows over active and reactive power. While the converter is usually limited to about 30 % of the rated power (since it is connected only to the rotor) it provides sufficient flexibility to control both active and reactive power/voltage independently within certain limits [10].

2.1.2 Type 4 Wind Turbine

The Type 4 wind turbine completely decouples the generator from the grid through its full power converter. Thus, the wind turbine can operate at an optimal speed while the converter synchronizes it with the grid [10]. The turbine has a generator-side converter which transforms the generated AC power to DC and a grid-side inverter which transforms DC to AC power and ensures that the turbine is synchronized to the grid. The generator, as shown in the overview of the Type 4 turbine in Figure 2.2, can be either an asynchronous generator or a permanent magnet synchronous generator, the latter being more common.

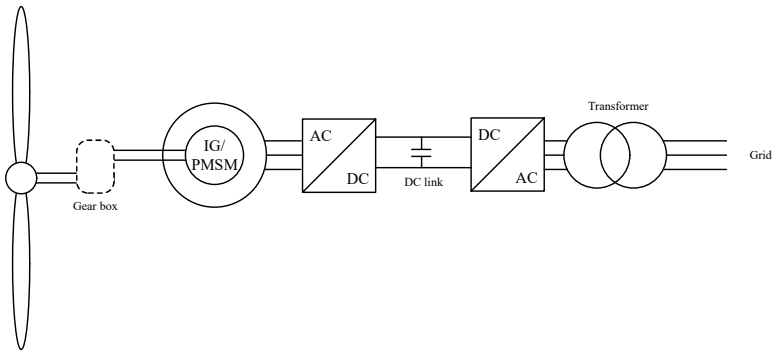

Figure 2.2: Overview key components Type 4 wind turbine

The full power converter allows for complete control of the active and reactive power/voltage output of the turbine, which is a significant advantage compared to previous turbine types. On the other hand, the increased losses within the converter, the higher cost, and the need for the converter to be rated for both active and reactive output are some of the main drawbacks of the Type 4 turbine [9].

2.2 Power System Stability

System stability is fundamental for the continuous and reliable delivery of electric power. In traditional power systems dominated by SGs, system stability was defined in [11] as the ability of the power system to return to its original operating state after a disturbance. However, the problem of stability is not singular. Instead, it is influenced by various types of dynamic behavior, such as rotor angle oscillations, frequency deviations, and voltage fluctuations. To capture the impact of these diverse factors, [11] introduced three classical stability classes: rotor angle stability, frequency stability, and voltage stability.

Each of the distinct classes covers a specific aspect of system stability. Rotor angle stability described the ability of SGs to maintain synchronization after a disturbance in the system [11]. This is tied to the balance between mechanical and electromagnetic torque in an SG, where instability can result in deviations in rotor angle or angular oscillations, which can cause loss of synchronization. Frequency stability, on the other hand, concerns the ability to maintain the nominal system frequency (50/60 Hz) in the face of disturbances that upset the equilibrium between load and generation [11]. Frequency stability relies on the system's ability to contain and restore frequency deviations with minimal load shedding. Failure to maintain system frequency can result in the loss of both generators and load. Voltage stability refers to the power system's ability to maintain steady voltages at all buses following a disturbance and is primarily driven by load characteristics and reactive power support to prevent voltage collapse. Instability in this context can lead to voltage collapse, resulting in load loss, equipment tripping, and potentially cascading outages.

With the continued integration of CBRs in the power system the dynamic behavior has changed [12], [13]. This has required power system stability to be revisited and expanded to capture the new behaviors caused by the integration of renewable energy sources in form of CBRs. A new classification of stability can be made according to Figure 2.3 [13], which represents a further development off the proposed classification in [11].

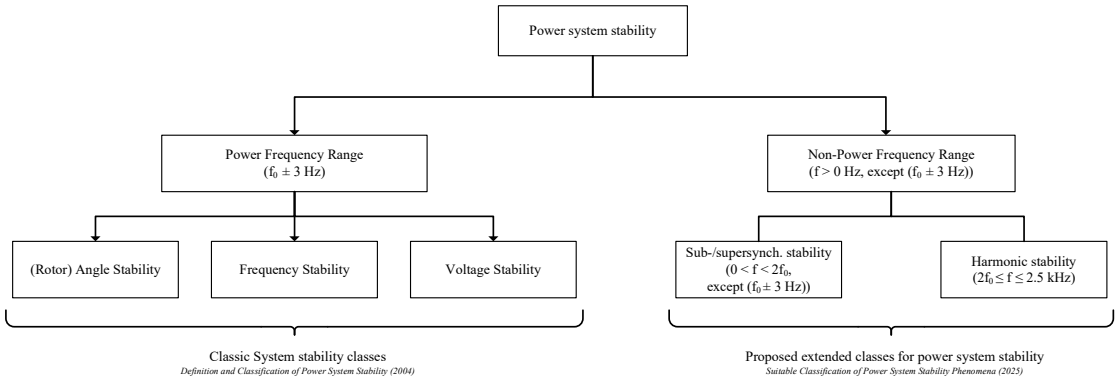

Figure 2.3: New classification of power system stability.

As shown in Figure 2.3, the classical stability classes introduced in [11] remain largely unchanged, with only minor adjustments made to what was previously termed rotor angle stability. These classes are grouped under the power frequency range, $f_0 \pm 3$ Hz, based on their original definitions, which were tied to an undistorted signal around the system's nominal frequency f_0 [13]. The adjustments to rotor angle stability include renaming it to angle stability to better encompass the phenomena exhibited by CBRs in the system. Unlike synchronous generators, CBRs do not synchronize to the grid through the same physical mechanisms but instead rely on alternative synchronization methods operating at the power frequency range. The behavior exhibited by these resources must be reflected in the revised definition of angle stability.

The second group of stability classes, introduced due to the changing dynamics of the power system, focuses on the non-power frequency range defined as frequencies $f > 0$, except $f_0 \pm 3$ Hz. This group contains two new stability classes: Sub-/supersynchronous stability and harmonic stability. Sub-/supersynchronous stability captures the behavior in the subsynchronous range $0 < f < (f_0 - 3)$Hz and supersynchronous frequency range $(f_0 + 3)\text{Hz} < f < 2f_0$ [13]. This class considers phenomena such as Sub-Synchronous Resonance (SSR), Sub-Synchronous Torsional Interaction (SSTI), and for CBRs in particular, Sub-Synchronous Control Interaction (SSCI). The second new stability class introduced in [13], Harmonic stability, captures phenomena in the frequency range $f \geq 2f_0$ up to frequencies of 2.5 kHz. Without proper damping, these interactions can lead to oscillations which, if their harmonic voltage or current exceeds protection thresholds, can lead to converter-based production being disconnected [13].

2.3 System Strength

System strength is frequently characterized by how much the voltage at a given point changes in response to a change in injected current [14], [15]. In essence, a system with robust or stiff voltage exhibits minimal voltage deviation in response to current disturbances. This is especially important for CBRs, for which the control system uses the voltage magnitude and angle to control power injection [15].

Assessing system strength is crucial for determining the maximum amount of power that can be reliably transferred during steady-state conditions, as well as for ensuring voltage stability in the long term. Within this framework, parameters like grid impedance and short circuit power are fundamental to understanding both system strength and the limits of power transfer, as will be described in the next section.

2.3.1 SCR: Traditional System Strength Estimation

System strength, has historically been evaluated based on short-circuit power. A high short-circuit power signifies that the system can maintain stable voltage levels even when subjected to current disturbances, which reflects a strong or stiff voltage profile.

To illustrate the relationship between short-circuit power and system strength, consider the simplified schematic shown in Figure 2.4. In this example, a CBR is connected to bus *i*, while the remainder of the network is represented by its Thévenin equivalent.

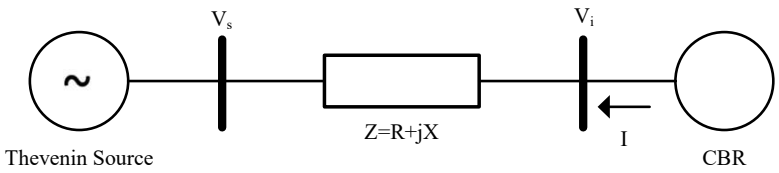

Figure 2.4: Connection of single CBR to Thévenin Equivalent representation of power system [16]

The voltage at the CBR's bus can be described as a function of the Thévenin voltage and the voltage drop across the network impedance:

$$V_i = V_s - Z \cdot I \tag{2.1}$$

For a small variation in the current supplied by the CBR, denoted ΔI, the corresponding change of voltage can be calculated as follows:

$$\Delta V_i + V_i = V_s - Z \cdot (I + \Delta I) \tag{2.2}$$

$$\Delta V_i = -Z \cdot \Delta I \Rightarrow Z = \Delta V / \Delta I \tag{2.3}$$

This demonstrates that Thévenin impedance is fundamentally related to the voltage change per unit change in current, a concept often referred to as voltage sensitivity. Voltage sensitivity is a key indicator of system strength. A large value of ΔV/ΔI implies that the bus voltage is highly sensitive to changes in injected current or power, which is typically described as a "weak bus" [16]. In such cases, the power introduced by the CBR can cause significant voltage fluctuations at bus *i*. Conversely, if the voltage is less affected by current variations, the system is considered strong.

Additionally, voltage sensitivity can be expressed in terms of short circuit power, S_{cc}, as shown in equation (2.4) and equation (2.5), where $I_{SC,i}$ is the short circuit current for a theoretical three-phase fault with zero impedance at bus i.

$$S_{cc} = \sqrt{3} \cdot V_i \cdot I_{SC,i} = \frac{V_i^2}{Z} \tag{2.4}$$

$$S_{cc} \propto 1/Z \propto \Delta I/\Delta V \tag{2.5}$$

This clearly establish the relationship between short-circuit power, voltage sensitivity, and system strength. Specifically, equation (2.4) and (2.5) highlight that short-circuit power is inversely proportional to both voltage sensitivity and Thévenin impedance. Therefore, buses with higher short circuit power values are typically classified as "strong," while those with lower short circuit power are considered "weak."

It is important to assess this strength relative to the power of the generating unit being connected. This is what the traditional measurement of system strength, SCR, does by normalizing the short circuit power, $S_{cc,i}$, with the rated active power, $P_{rated,i}$ of the connected plant at bus i. It is defined as follows:

$$SCR_i = \frac{S_{cc,i}}{P_{Rated,i}} \tag{2.6}$$

Given that SC is calculated as in equation (2.4), if the base power of the system is set equal to $P_{rated,i}$ and V_i is assumed to be 1 pu, SCR can be calculated with the Thévenin impedance of bus i, $Z_{pu,i}$ as follows [10]:

$$SCR = \frac{S_{cc,i}}{P_{Rated,i}} \Rightarrow \frac{V_{pu,i}^2/Z_{pu,i}}{P_{pu,i}} \Rightarrow \frac{1}{Z_{pu,i}} \tag{2.7}$$

One aspect which is important when discussing system strength and SCR, is the point at which the system strength is estimated. Usually system strength is discussed in terms of the High Voltage/Point of Connection (HV)/(POC), or the Medium Voltage (MV) bus [8]. The only difference is the point at which the short circuit power or Thévenin impedance is calculated. An illustration of these points can be seen in Figure 2.5.

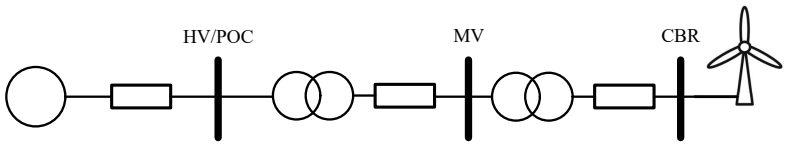

Figure 2.5: Illustration of POC and MV-busF [10]

Due to the impedance of the transformers and overhead lines (OH-lines) or cables between the MV-bus and the POC the SCR_{MV} will be reduced compered to SCR_{POC}. The thresholds according to [8] are defined below, but in this project the calculated system strength measurements will be presented for the MV bus.

- Strong system: $SCR_{POC} > 5$, $SCR_{MV} > 4$
- Weak system: $3 < SCR_{POC} < 5$, $2 < SCR_{MV} < 4$
- Very weak system: $SCR_{POC} < 3$, $SCR_{MV} < 2$

According to [17], these thresholds for SCR originate from the introduction of Line-Commutated Converter (LCC) HVDC applications and have continued to be utilized, as most manufacturers today specify a minimum SCR of 3 at the HV/POC for their converters. However, some manufacturers now guarantee operation at a minimum SCR of less than 3, meaning that exceptions can be made for individual types of converters.

2.4 System Strength for CBR Integration

The integration of CBRs has heightened the importance of system strength within modern power systems. CBRs rely on Phase-Locked Loops (PLLs) for system synchronization, which require precise detection of voltage angle and frequency. Unlike traditional synchronous generators, CBRs exhibit greater sensitivity to the voltage waveform at their connection point. In environments characterized by low system strength, the current supplied by CBRs can significantly alter the local voltage profile, potentially triggering control system oscillations or instability [18].

Addressing stability challenges in senarios with low system strength scenarios does not always necessitate extensive grid reinforcement. In many instances, refining the control strategies, such as the PLL of the CBRs themselves offers a more practical approach to maintaining stable operation under weak-grid conditions [19]. By carefully adjusting control parameters, CBRs can be operated safely even as the system approaches lower SCR thresholds.

Nevertheless, the reliability of SCR as an indicator of system strength in contemporary power networks is increasingly debated. This debate arises primarily from the transition from predominantly synchronous generation to systems with a higher proportion of converter-based generation. As a result, several new system-level metrics have been introduced to better reflect the characteristics of modern power systems. System strength metrics designed to address CBR control interactions and oscillations can be classified in three groups: impedance-based analysis, interaction factors and SCR-based methods. These groups have subdivisions in which the core idea remains the same but the implementation differs. A high-level breakdown of this classification is presented in Figure 2.6 below. The Available Fault Level (AFL) is included as a separate category from SCR since, even though it relies on short circuit power, the core idea of the metric is different.

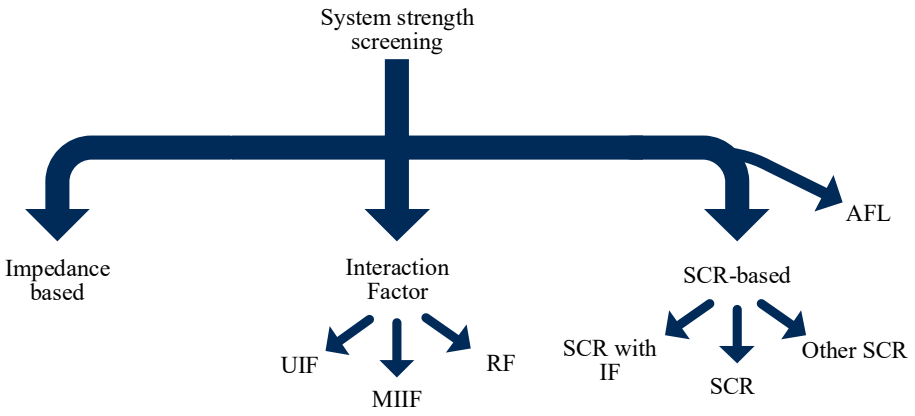

Figure 2.6: Overview of the main types of measurements of system strength

2.5 Impedance-Based Analysis

Impedance-based analysis of system stability allows for detailed results but comes at the cost of high data requirements and complexity. While these requirements have placed the impedance-based analysis outside the scope of this thesis, a brief overview can provide valuable insight and help understand other metrics for evaluating system stability and strength.

The impedance-based stability analysis in [20] uses the frequency dependent grid impedance and the converter admittance to analyze small signal system stability. The frequency dependent grid impedance is assumed to be available through a frequency scan of the modeled grid. This can for example, be accomplished in the simulation environment PSS®E using the harmonics module.

The frequency dependent converter admittance can be obtained through a frequency scan of the converter EMT model. The method used in [20] is based upon the work in [21]. The frequency scan is conducted by the introduction of a voltage perturbation, with frequency f_p, in the positive and negative sequence voltage. These are represented as $\hat{v}_p(f_p)$ and $\hat{v}_n(f_p)$, and result in a response $\hat{i}_a(f_p)$ from the converter. Given $\hat{v}_p(f_p)$, $\hat{v}_n(f_p)$ and $\hat{i}_a(f_p)$ the self impedances and coupling term impedances can be calculated for positive and negative sequence according to equation (2.8) where f_1 is the nominal frequency of the system.

$$Z_{ap} = \frac{\hat{v}_p(f_p)}{\hat{i}a(f_p)} \quad Z_{an} = \frac{\hat{v}_n(f_p)}{\hat{i}a(f_p)} \quad Z_{cp} = \frac{\hat{v}_p(f_p)}{\hat{i}a(f_p - 2f_1)} \quad Z_{cn} = \frac{\hat{v}_n(f_p)}{\hat{i}_a(f_p + 2f_1)} \tag{2.8}$$

Given the relationship between $\hat{v}_p(f_p)$/ $\hat{v}_n(f_p)$ and $\hat{i}_a(f_p)$ illustrated in Figure 2.7.

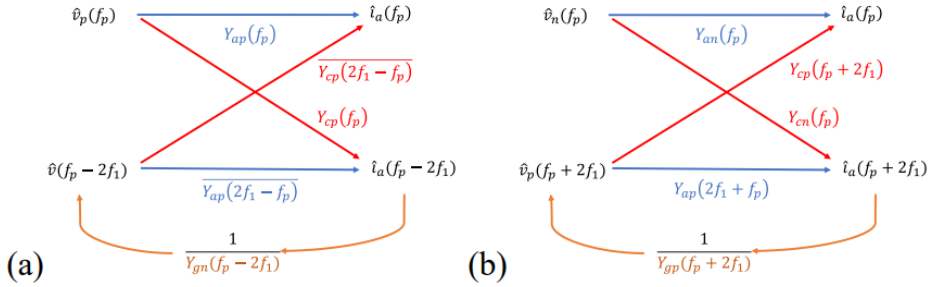

Figure 2.7: The resulting chain reaction due to introduced voltage perturbation for a) positive sequence and b) negative sequence [20]. Reprinted with permission.

The positive and negative sequence converter admittances, $Y_p(f_p)$ and $Y_n(f_p)$ can be obtained by equation (2.9) and equation (2.10), where Y_{gp} and Y_{gn} are the positive and negative sequence grid admittances.

$$Y_p(f_p) = Y_{ap}(f_p) - \frac{\overline{Y_{cp}(2f_1 - f_p)} \cdot Y_{cp}(f_p)}{\overline{Y_{ap}(2f_1 - f_p)} + Y_{gn}(f_p - 2f_1)} \tag{2.9}$$

$$Y_n(f_p) = Y_{an}(f_p) - \frac{Y_{cp}(f_p + 2f_1) \cdot Y_{cn}(f_p)}{Y_{ap}(f_p + 2f_1) + Y_{gp}(f_p + 2f_1)} \tag{2.10}$$

The positive sequence admittance $Y_p(f_p)$ can then be used to obtain the representation of the frequency dependent converter impedance, $Z_{p,c}(f_p)$, according to equation (2.11).

$$Z_{p,c}(f_p) = \frac{1}{Y_p(f_p)} \tag{2.11}$$

A Bode plot of the amplitude and phase of the grid and converter impedance can then be evaluated. If the amplitude of $Z_{p,c}(f_p)$ and $Z_g(f_p)$ match with negative damping, the resonance will remain undamped, which leads to system instability. However, the Bode plot will only show if the respective impedance profiles match. For a conclusive result regarding damping and stability the Nyquist plot needs to be evaluated [20].

2.6 SCR-Based System Strength Metrics

A variety of alternative SCR-based metrics have been developed for system strength screening. This section provides an overview of the most established metrics, outlining their principles of operation, strengths, and limitations.

2.6.1 Weighted Short Circuit Ratio

Weighted Short Circuit Ratio (WSCR) was developed by Electric Reliability Council of Texas (ERCOT) to detect the risk of voltage oscillations due to interaction between CBRs [22]. It is formulated under the assumption that all resources within a defined area of the grid are fully interacting, effectively behaving as if connected

to the same electrical point. To reflect this, WSCR incorporates a weighting factor to account for the effect this interaction has on system strength. The metric is described in [22] as:

$$WSCR = f_w \cdot \frac{S_{cc}}{\sum P_{rated,i}} = \frac{\sum(S_{cc,i} \cdot P_{rated,i})}{(\sum P_{rated,i})^2} \tag{2.12}$$

where f_w is the weighting factor, $S_{cc,i}$ is the short circuit power at bus i without the plant connected, and $P_{rated,i}$ is the rated active power at bus i.

WSCR was originally designed for and applied to a cluster of wind farms in the Panhandle region of Texas [22]. This part of the electrical grid was relatively isolated from the rest of the grid with only two lines connecting it to the main grid [22]. Previous experience showed that the disconnection of either line significantly reduced system strength, increasing the likelihood of voltage oscillations. To mitigate this, WSCR was designed with these specific conditions in mind. In such cases, it is reasonable to make the assumption of electrical closeness between wind farms and this justifies why WSCR uses full interaction. However, this modeling choice also makes WSCR a more conservative metric compared to other SCR-based approaches. Rather than evaluating the contribution of each unit separately, WSCR assesses the system strength of the entire group collectively.

For real world application, WSCR is used as a real-time monitoring tool in the Panhandle region [8], continuously assessing system strength based on live grid conditions and actual wind farm output rather than rated power [23]. A WSCR threshold of 1.5 is used to indicate stable operation. If the value drops below this threshold, output from the wind farms is curtailed to maintain system stability [23].

2.6.2 Composite Short Circuit Ratio

Established by General Electric in 2015 as an alternative measurement to SCR to account for the interaction of CBRs [24]. Composite Short Circuit Ratio (CSCR) was primarily aimed at the medium voltage collection grid which connects multiple CBRs within a wind farm [10]. According to [8] CSCR creates a fictitious bus which all CBR-buses are connected to. The fictitious bus is connected to the grid by the original connections of each CBR in parallel. This can be seen in Figure 2.8

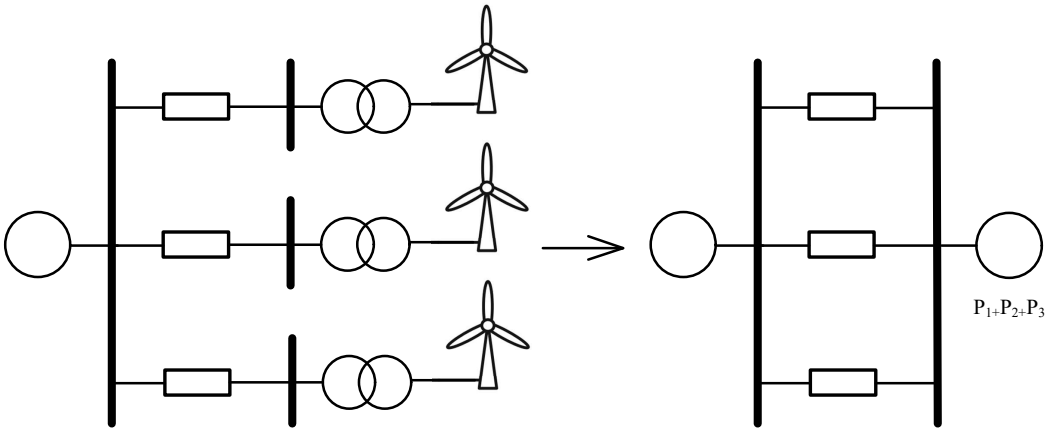

Figure 2.8: Overview of CSCR

The CSCR of the system can then be calculated as for SCR, but with the short circuit power of the fictitious bus, $S_{cc,fic}$, and the sum of rated active power, $\sum P_{rated,i}$, of the CBRs connected to the fictitious bus.

$$CSCR = \frac{S_{cc,fic}}{\sum P_{rated,i}} \tag{2.13}$$

CSCR gives one estimation of system strength for all CBRs which are considered, and as for WSCR it can not estimate system strength at individual busses. The primary objective of CSCR is to provide an aggregated system strength estimation for wind turbines connected in wind farm.

2.6.3 Equivalent Short Circuit Ratio

Equivalent Short Circuit Ratio (EqSCR), also referred to as SCR with Interaction Factor (SCRIF), is a system strength evaluation metric that accounts for the interaction between CBRs [8], [15]. This is achieved by introducing a penalty factor, which aggregates rated active power multiplied with a Multi-Infeed Interaction Factor (MIIF) for all other CBRs connected in the system [10], [8]. The metric is defined by the following equation 2.14,

$$EqSCR_i = \frac{S_{cc,i}}{P_i + \sum(\text{MIIF}_{ji} \cdot P_j)} \tag{2.14}$$

where $S_{cc,i}$ is the short circuit power at bus i, P_i is the rated active power of the CBR at bus i, MIIF_{ji} is the interaction factor between buses j and i, and P_j is the rated active power of the CBR at bus j.

The interaction factor, MIIF, estimates the risk of electrical interaction between two CBRs. It is determined by introducing a small voltage perturbation at one bus and measuring the voltage response at other buses. A more detailed explanation of the

MIIF calculation is provided in Sections 2.8.2 and 2.8.3, but the interaction factor MIIF_{ji} is defined as:

$$\text{MIIF}_{ji} = \frac{\Delta V_j}{\Delta V_i} \tag{2.15}$$

where ΔV_i is a voltage change introduced at bus i and ΔV_j is the resulting voltage change at bus j.

2.6.4 Site-Dependent Short Circuit Ratio

Site-Dependent Short Circuit Ratio (SDSCR) is similar to EqSCR in that it uses a penalty factor to improve the estimation of system strength. However, SDSCR uses an impedance-based interaction factor which considers the impedance between the buses with CBRs and is defined as follows in [8] and [25]:

$$SDSCR_i = \frac{|V_{R,i}|^2}{\left(P_{R,rated,i} + \sum_{j \in R, j \neq i}(P_{R,rated,j,} \cdot \omega_{ij})\right)|Z_{R,ii}|} \tag{2.16}$$

where R is the set of buses with CBR in the system, $V_{R,i}$ is the voltage at bus i in R, $P_{R,rated,i}$ and $P_{R,rated,j}$ is the rated active power of the CBR at respective bus, $Z_{R,ii}$ the Thévenin impedance at bus i and ω_{ij} the electrical interaction factor between bus i and j. The electrical interaction factor is defined as:

$$\omega_{ij} = \frac{Z_{R,ij}}{Z_{R,ii}} \cdot \overline{\left(\frac{V_{R,i}}{V_{R,j}}\right)} \tag{2.17}$$

with V_R, j as the voltage on bus j and $Z_{R,ij}$ the impedance between the bus i and j in the set R.

2.6.5 Effective Short Circuit Ratio

Effective Short Circuit Ratio (ESCR) was developed for integration of LCC HVDC devices [8]. It is a simple evolution of SCR to account for the use of shunt capacitors at the terminal of HVDC terminals, which was found to increase the effective impedance of the system [26]. To account for this the reactive shunt compensation is removed from the original short circuit power when ESCR is calculated as in equation (2.18) according to [27]:

$$ESCR_i = \frac{SC_{cc,org,i} - Q_i}{P_{rated,i}} \tag{2.18}$$

Where $S_{cc,org,i}$ is the short circuit power without the shunt connected, Q_i is the reactive power from the shunt and $P_{rated,i}$ is the active power of the plant at the bus, all at the designated bus i.

However, it should be noted that traditional SCR can account for the addition of shunt compensation. This is examined thoroughly in [27] where the voltage stability

limit of a single converter system with shunt compensation is evaluated similar to Figure 2.9.

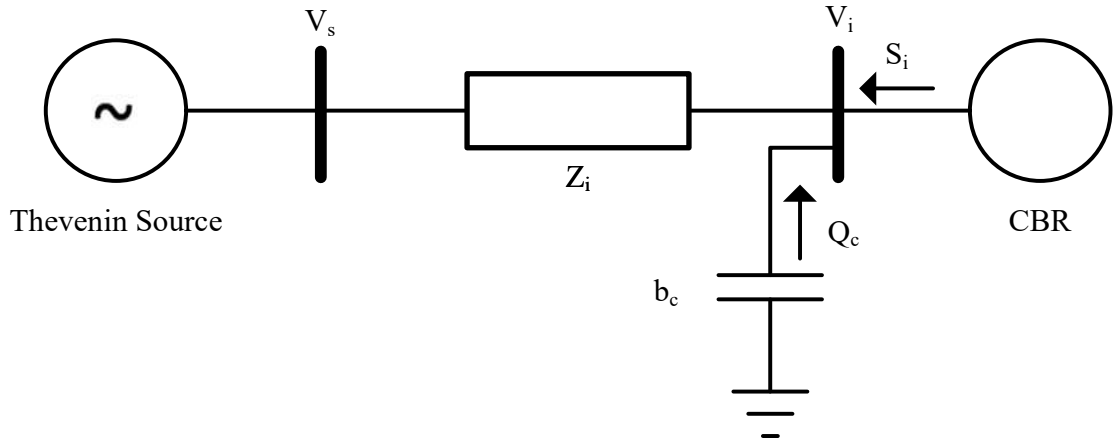

Figure 2.9: Single CBR with shunt compensation [27]

A detailed breakdown of the voltage stability analysis is available in [27], but the boundary condition r_i of the analysis can be broken down and represented as:

$$r_i = \frac{|V_i|^2}{|\overline{S_i}| \cdot |Z_i'|} = \frac{|S_{ac,i}'|}{|\overline{S_i}|} = \frac{\left|\frac{|V_i|^2}{Z_i'} - j\frac{|V_i|^2}{X_C}\right|}{|\overline{S_i}|} = \frac{|SC_{ac,i} - jQ_{c,i}|}{|\overline{S_i}|} = 1 \tag{2.19}$$

where V_i is the voltage at bus i, Z_i and Z_i' are the Thévenin impedance without and with consideration of the connected shunt compensation, X_c is the capacitive reactance of the shunt compensation and $\overline{S_i}$ is the conjugate of the complex apparent power injected by the CBR.

What equation (2.19) demonstrates is that the presence of shunt compensation must be considered when evaluating system strength, in order to avoid overestimation. However, this can be addressed either by using ESCR, with the original short circuit power $SC_{ac,i}$ and the reactive power $Q_{c,i}$, or by recalculating the short circuit power $SC_{ac,i}'$ to reflect the change in system impedance introduced by the shunt compensation.

2.6.6 Multi-Infeed Effective Short Circuit Ratio

Multi-Infeed Interaction Factor (MIESCR) was developed as a metric for system strength, which could account for the impact of the growing amount of LCC HVDC stations [28]. MIESCR is based on ESCR and incorporates Q-compensation in the same manner as ESCR. To account for interaction, MIESCR utilizes MIIF, to scale the contribution from other LCC HVDC links within the system. The full metric can be defined as follows by [28]:

$$MIESCR_i = \frac{S_{cc,org,i} - Q_i}{P_i + \sum(MIIF_{ji} \cdot P_j)} \tag{2.20}$$

Where $S_{cc,org,i}$ is the short circuit power without the connection of shunt compensation and Q_i is the reactive power compensation at bus i. P_i and P_j is the nominal active power of LCC HVDC connected at bus i and j respectively, while $MIIF_{ji}$ is the interaction factor between the same buses i and j as described in equation (2.14).

MIESCR and EqSCR are similar in that both use the interaction factor to account for the influence of multiple units on one another. EqSCR, defined in 2016 in [10], can be considered a simplification of MIESCR, which was introduced earlier in 2008 in [28]. The key distinction lies in the way MIESCR uses short circuit power which does not account for the impact of the shunt compensation while EqSCR can be calculated with a short circuit power which does account for this. This is similar to how SCR and ESCR are related as seen in Section 2.6.5, thus making MIESCR somewhat superfluous if tools are available to easily calculate an updated short circuit power for EqSCR.

2.6.7 Interactive Short Circuit Ratio

Interactive Short Circuit Ratio (ISCR) is a development of SDSCR to account for Static Var Compensation (SVC), on the bus which the CBR is connected to [17]. It can be defined as in equation (2.21) according to [8]:

$$ISCR_i = \frac{\left| \frac{V_{R,i}^2}{Z_{R,ii}} + j\frac{V_{R,i}^2}{X_{svc,i}} \right|}{\left| S_{R,rated,i} + \sum_{j \in R, j \neq i} (S_{R,rated,j,} \cdot \omega'_{ij}) \right|} \tag{2.21}$$

where R is the set of buses with CBRs connected, $S_{R,rated,i}$ and $S_{R,rated,j}$ represent the rated apparent power of the CBRs on bus i and j, and $X_{svc,i}$ is the reactance of the SVC at bus i. $Z_{R,ii}$ is the Thévenin impedance of bus i without the SVC connected and $V_{R,i}$ is the voltage at bus i. ω'_{ij} is the updated interaction factor between bus i and j and can according to [8] be defined as:

$$\omega'_{ij} = \overline{\left(\frac{Z'_{R,ij}}{Z'_{R,ii}} \right)} \cdot \frac{V_{R,i}}{V_{R,j}} \tag{2.22}$$

with V_R, j and V_R, j the voltage at the respective bus, $Z'_{R,ii}$ and $Z'_{R,ij}$ and are the Thévenin impedance and the impedance between the bus i and j in the set R.
The main point of ISCR is how the metric is a development of SDSCR to account for the effects of SVC on system strength. ISCR uses $V_{R,i}^2/Z_{R,ii}$ and $V_{R,i}^2/Z_{SVC,i}$ this can be viewed as the reactive power without the SVC connected and and the reactive power of the shunt. Compered to $V_{R,i}^2/Z_{R,ii}$ of SDSCR which is the short circuit power. This is similar to how ESCR and SCR are related as well as how EqSCR and MIESCR are related. Based on what was seen in Section 2.6.5 it is clear how SCR can account for shunt compensation if updated parameters are used and this makes ISCR redundant to SDSCR.

2.6.8 Inverter Interaction Level Short Circuit Ratio

Inverter Interaction Level Short Circuit Ratio (IILSCR) is another alternative to SCR which tries to account for CBR interaction. IILSCR models the interaction by using the load flow between CBR buses and it calculates the IILSCR by summing the active power at bus i with active power flowing to bus i from other buses with CBRs [29].

$$IILSCR_i = \frac{S_{cc,i}}{P_{rated,i} + \sum_{j=1,j\neq i}^{n} P_{ij}} \tag{2.23}$$

where P_{ij} is the load flow from bus j to bus i. The main drawback of IILSCR is the use of power flow in the system, which is usually driven by load. The other methods for evaluating interaction have tried to quantify how close the CBRs are electrically. However, a large power flow does not necessarily mean that there is a large interaction between the CBR at two busses. For example, it could be that one bus has a large load which will result in a large power flow to this bus.

2.7 Available Fault Level

AFL is another short circuit based measurement but is distinct from other SCR-based methods. The method considers that synchronous generators provide short circuit power, referred to as fault level. CBRs such as wind, solar or HVDC-devices on the other hand are considered to absorbs short circuit power[30]. If there is no short circuit power available at a bus, then the fault level is negative, which indicates potential instability, and triggers the criteria for further detailed studies. AFL can either be considered for one single bus or a collection of close by buses with multiple CBRs.

To calculate the AFL at a designated bus, the following steps are to be followed.

1. Calculate the fault level with only synchronous generators connected, FL_{sg} .
2. Calculated required fault level, FL_{req} if there are already connected CBRs.

   $$FL_{req} = MSCR_{ex} \cdot P_{rated} \tag{2.24}$$

   Where P_{rated} is the rated active power of the CBR and $MSCR_{ex}$ is the minimum SCR, MSCR, of the existing CBR. MSCR refers to the lowest SCR level the CBR can be connected to without any instability occurring.
3. Calculate AFL at the bus for any new CBR

   $$AFL = FL_{sg} - FL_{req} \tag{2.25}$$

4. Once the AFL is calculated, the maximum power rating without causing instability for the intended CBR to be connected at the studies bus can be calculated as follows

   $$P_{rated,new} = \frac{AFL}{MSCR_{new}} \tag{2.26}$$

Where $P_{rated,new}$ is the rated power of the planned CBR and and $MSCR_{new}$ is the minimum SCR of the converter.

To calculate the AFL at a designated bus i, with CBRs connected close by in the system, the method is changed as below.

1. Calculate fault level, FL_{SG} with only synchronous generators connected. This represents the available short circuit power at the bus.

2. Calculate total fault level FL_{tot} at each bus, with the connected CBR represented by a Thévenin voltage source and an effective impedance, Z_e

$$Z_e = \frac{V^2}{MSCR \cdot P_{rated}} \tag{2.27}$$

   Where V is the voltage at the bus the CBR is connected to, $MSCR$ the minimum SCR of the connected CBR and P_{rated} the rated power of the CBR.

3. Calculate the estimation of absorbed short circuit power, fault level, as the difference between the FL_{SG} and and FL_{tot}

$$\Delta FL = FL_{tot} - FL_{SG} \tag{2.28}$$

4. Finally calculate the AFL as the difference between available short circuit power and estimated absorbed short circuit power:

$$AFL = FL_{SG} - \Delta FL \tag{2.29}$$

AFL has according to [30] been used to screen planed connections of CBRs by the Australian Energy Market Operator (AEMO) since 2018. This has brought some insights to the difficulties and strengths of the AFL measurement. Especially the importance of the MSCR has been highlighted. When AFL was first applied no MSCR was available for older connections. This lead to that the standard value of MSCR 3 was used, which is in line with the traditional threshold for strong and weak system. However, this very conservative estimation of MSCR resulted in negative AFL and triggered EMT studies that were found to be unnecessary in many cases. From experienced gained by these EMT studies it was found that a MSCR of about 2 was applicable in most cases including for already existing CBRs.

2.8 Interaction Factors

Interaction factors are designed to quantify the risk of interaction between two devices within the system. If an additional device is connected in the system, the interaction factor between the original two devices does not consider the third device or the effects of the aggregated risk of interaction among multiple devices.

System strength, however, aims to provide an aggregated overview of various factors that affect power system stability, which renders interaction factors unsuitable for this particular purpose. Nevertheless, interaction factors have proven useful in metrics such as EqSCR and SDSCR for estimating the effects that multiple CBRs have on system strength. Therefore, it is important to understand the underlying theory of interaction factors for system strength estimation.

2.8.1 Unit Interaction Factor

Unit Interaction Factor (UIF) approximates the risk of SSTI between a LCC HVDC-link and a generator [8]. It is a simple measurement in its use of only positive sequence components to accomplish this. It is defined by [8] as:

$$UIF_i = \frac{S_{HVDC}}{S_{Gen}} \cdot \left(\frac{Y_{12}}{Y_{11}}\right)^2 \tag{2.30}$$

Where Y_{12} is the admittance between internal bus for generator and HVDC terminal. Y_{11} is the admittance from HVDC to rest of system.

UIF is primarily intended for the screening of SSTI between LCC HVDC systems and generators. The threshold for when further studies are recommended is found to be at 0.1. This threshold has been established when the method was first developed in the 1970s [31]. Since then, it has been extended to include VSC HVDC applications. However, due to the fundamental differences between LCC and VSC technologies, additional investigations are required to validate its applicability in such cases [8].

The primary focus of this thesis is the effect caused by converter-based production on system strength. As seen in Section 2.6 many SCR-based metrics utilize some kind of IF to estimate the aggregated effect of the surrounding CBRs. Thus, a variant of UIF applied to estimate interaction between CBRs could be of interest. Such converted variant of equation (2.30) could be defined as:

$$UIF_{ji} = \frac{S_i}{S_j} \cdot \left(\frac{Y_{ij}}{Y_{ii}}\right)^2 \tag{2.31}$$

where S_i and S_j is the apparent power of the CBR at the respective bus, Y_{ij}, the admittance between the two CBRs and Y_{ii} the admittance between CBR at bus i and the rest of the system.

2.8.2 Classical Multi-Infeed Interaction Factor

To estimate the interaction between two LCC HVDC systems, the Classical Multi-Infeed Interaction Factor (CMIIF) was introduced in 2008 [8]. In [28], the AC bus voltage of a converter is noted as the most representative parameter for assessing the interaction between HVDC converters. Based on this, the MIIF was defined as the ratio between an introduced voltage dip, ΔV_i, at bus i and the resulting voltage

dip, ΔV_j, at bus j:

$$MIIF_{ji} = \frac{\Delta V_j}{\Delta V_i} \tag{2.32}$$

This voltage dip is typically introduced as a step change with an amplitude of approximately 1 %, this can be accomplished by introducing and switching a fixed shunt reactance. For electrically close buses, the MIIF will approach one since the voltage drop will be similar, whereas for electrically distant buses the resulting voltage dip at bus j will be much smaller and MIIF will approach zero.

Different sizes of HVDC devices will allow the converter to affect devices differently. Since HVDC converters may differ significantly in size, the degree of influence they exert on one another also varies. To capture this behavior a weighted CMIIF is often used which considers the size of both converters.

$$CMIIF_{w,ji} = \frac{\Delta V_j}{\Delta V_i} \cdot \frac{P_{\text{HVDC,i}}}{P_{\text{HVDC,j}}} \tag{2.33}$$

Where $P_{\text{HVDC,i}}$ and $P_{\text{HVDC},j}$ represent the rated active power of the HVDC devices connected at their respective buses. A weighted CMIIF below 0.15 can according to [28] be seen as low risk for interaction. If it increases to between 0.15 and 0.4 the risk would be classified as moderate and finally above 0.4 the risk can be deemed to be high.

2.8.3 Extended Multi-Infeed Interaction Factor

Extended Multi-Infeed Interaction Factor (EMIIF) is an adaptation of CMIIF aimed at VSC-based HVDC rather than LCC HVDC. There are two types of EMIIF, calculated with the traditional use of voltage amplitude and EMIIF calculated with voltage angle difference [8]. The angle EMIIF is different in that it uses the change of angle caused by a voltage dip rather than change of amplitude. To be able to calculate this a voltage step with a resistive shunt is applied. The angle-based EMIIF can be calculated as:

$$EMIIF_{ang,ij} = \frac{\delta_j}{\delta_i} \tag{2.34}$$

Where δ_j and δ_i are the change of angle for the voltage at bus i and j caused by the switched shunt resistance.

The difference in amplitude EMIIF compared to CMIIF lies in the use of rated reactive power instead of active power when applying the weighting to account for the size of devices. This is meant to allow weighted EMIIF to better account for the behavior of VSC in contrast to CMIIF, which was originally designed for LCC HVDC.

The use of active power in CMIIF is reasonable because, for LCC HVDC systems, reactive power is directly related to active power, typically with a ratio of $Q/P =$ 0.5–0.6 [8]. A change in voltage which requires a change of reactive power would therefore force a change of active power as well. For VSC however the reactive power

is decoupled from the active power. A change in voltage only requires the reactive power to change. Thus, Weighted amplitude EMIIF considers reactive power and is defined as:

$$EMIIF_{w,ji,\text{amp}} = \frac{\Delta V_j}{\Delta V_i} \cdot \frac{Q_i}{Q_j} \tag{2.35}$$

Where Q_i and Q_j are the rated reactive power of the VSC at their respective bus while ΔV_j and ΔV_i is the voltage dip introduced by a reactive shunt at bus i.

The change in voltage angle is instead tied to the active power. Therefore, the angle EMIIF, similar to CMIIF, uses the active power of the CBRs when weighted [8]. The Weighted angle EMIIF can be defined as:

$$EMIIF_{w,ji,\text{ang}} = \frac{\delta_j}{\delta_i} \cdot \frac{P_i}{P_j} \tag{2.36}$$

Where P_i and P_j are the rated active power of the VSC at their respective bus while δV_j and δV_i is the change in voltage angle introduced by a resistive shunt at bus i.

The thresholds for weighted EMIIF remain the same as for CMIIF, this mean risk of interaction is considered low below 15%, moderate between 15% and 40% and high above 40% [8].

2.8.4 Radiality Factor

When first defined in, [32], Radiality Factor (RF) was used as an indicator of the risk of interactions between a generator and other dynamic devices in the sub-synchronous frequency spectrum. It has later been extended in [31] to identify the risk of interaction between two dynamic devices based on the electrical closeness between those devices. RF is distinguished from many other screening methods in its use of grid impedance in the sub synchronous frequency range to determine the electrical distance. Contrary to many other measurements that require frequency dependent impedance data RF does not require any converter impedance in the assessment. The grid impedance in the sub-synchronous frequency range is usually known at an early stage to system planners. This allows RF to be used as a screening method when other impedance methods have been excluded.

To calculate the RF between two buses, the system has to be reduced to the two buses of interest. The admittance can the be used to calculate the RF at frequency f as follows

$$RF_{ij,f} = \frac{2 \cdot |Y_{12,f}|}{|Y_{1G,f}| + |Y_{2G,f}| + 2 \cdot |Y_{12,f}|} \tag{2.37}$$

where $Y_{12,f}$ is the admittance between the two buses and $Y_{1G,f}$, $Y_{2G,f}$ are the equivalent addmitances between the device and ground. The 2x2 admittance matrix between the devices can be defined as in equation (2.38)

$$Y_f = \begin{bmatrix} Y_{1G,f} + Y_{12,f} & -Y_{12,f} \\ -Y_{12,f} & Y_{1G,f} + Y_{12,f} \end{bmatrix} \tag{2.38}$$

In [32], a threshold value of 0.2 at torsional frequencies is identified as the point at which the risk of torsional instability warrants consideration. However, [31] notes that this threshold is based on a very limited set of tests. It is therefore suggested that the worst-case scenario should always be evaluated directly; if stability is confirmed under this condition, stable operation can be expected at other frequencies as well. Additionally, the RF can be calculated at 50 Hz when it is intended to be used as an interaction factor similar to MIIF in the EqSCR metric.

3
Method

This chapter presents the methodology employed in this thesis. First, the traditional system strength metric, namely the SCR, is assessed within the context of converter-dominated power systems. This assessment highlights the limitations of SCR and underscores the need for more robust grid strength metrics.

Next, alternative system strength metrics described in chapter 2 are examined through a series of small-scale case studies. These case studies serve a pedagogical purpose, providing an initial understanding of these metrics and enabling the rapid identification of their respective advantages and disadvantages. This approach facilitates the selection of the most promising metrics for subsequent comprehensive evaluation.

Finally, the metrics identified in the previous step are implemented in PSS®E and validated against detailed simulations conducted in PSCAD. The accuracy of these metrics is verified through this process, allowing for the determination of the most suitable alternative system strength metric for effective screening during the early stages of grid planning. Note that this chapter describes the methodology, while the results and discussion are presented in Chapters 4 and 5, respectively.

3.1 Evaluation of Traditional System Strength

To evaluate the traditional system strength i.e SCR, several simulations in PSCAD were performed. The simulations were specifically designed to highlight the limitations of SCR. These investigations demonstrate how instabilities can arise from phenomena occurring outside the fundamental frequency of 50 Hz, which SCR is not well-equipped to detect. Furthermore, the results illustrate the impact of multiple CBRs within the system and the inability of SCR to reliably capture their impact on system strength.

3.1.1 SCR in Single Converter System

This evaluation was performed on a simplified system in which a wind farm composed of Type 4 wind turbines was connected to a system modeled by an RL circuit with programmable resistance and inductance values. These parameters were gradually varied, from conditions representing a high SCR to low SCR, with the objective of identifying the SCR threshold at which the wind farm loses stability under full

power injection. Instability is expected to occur under weak grid conditions, typically when SCR < 2. The setup is illustrated in Figure 3.1.

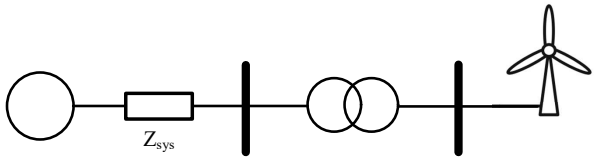

Figure 3.1: Simple circuit with converter-interfaced generation in wind farm

To simulate the Type 4 wind farm in EMT simulation, PSCAD´s openly available Type 4 wind turbine generator was used. The technical documentation is available in [33]. The relevant parameters of the Type 4 simulation block are presented in Table 3.1. The Type 4 model has a voltage control mode that maintains voltage by controlling reactive power output. In addition to voltage control, the model was supplemented by introducing a simple reactive control mode, where the reference value for the wind farm´s reactive power output was set to a fixed level. However, for this project the Type 4 model was used in voltage control mode.

Table 3.1: Parameters for Type 4 wind turbine model

Parameter	Value
Cut-in Wind speed	3 m/s
Rated wind speed	10 m/s
Cut-out Wind speed	25 m/s
Turbine S_{rated}	2 MVA
Turbine Q_{max}	1.3 MVAr

To better understand the nature of the instability introduced by reduced system strength, a frequency-domain impedance-based analysis described in Section 2.5 was conducted. This analysis was performed for two operating points at which the converter was stable and unstable, respectively.

3.1.2 SCR in Series Compensated System

The issue of instability with CBRs becomes increasingly problematic in the presence of series compensation. To evaluate the effect of series compensation on system stability two cases were considered. The first case, illustrated in in Figure 3.2 assumes that connecting lines are series compensated, and in the second case an uncompensated line is connected in parallel with the compensated line. Similar to the system in Section 3.1.1, the impedance was modeled as programmable R, L and C values. This allows the resistance and inductance to be adjusted to match a

predefined SCR for the connected wind farm. Similarly, the capacitance could be changed to account for a certain level of series compensation.

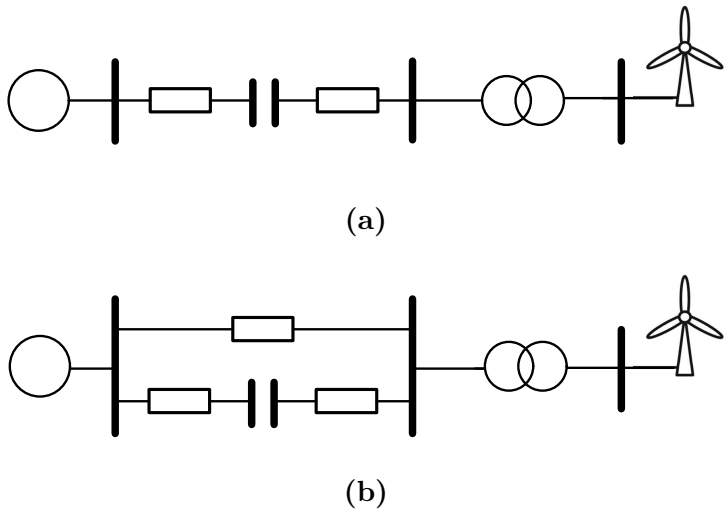

Figure 3.2: System configurations with series compensation: (a) Radially connected wind farm, (b) An additional uncompensated line connected in parallel

Simulations for these two cases were performed with a Type 3 wind farm with a rated power of 200 MW connected. For this, PSCAD´s openly available model was used, with the technical documentation available in [34]. The base model is configured to have a power factor of 1 and no reactive power exchange with the grid. To enable the model to operate in voltage control mode or reactive power control, the control system was modified. Each turbine in the simulation model can provide 5 MW, and similar to the Type 4 model the model can scale production by adjusting the number of turbines.

Table 3.2: Parameters for Type 3 wind turbines model

Parameter	Value
Cut-in Wind speed	3 m/s
Rated wind speed	11 m/s
Cut-out Wind speed	25 m/s
Turbine P_{rated}	5 MW

In the simulations prior to the introduction of any series compensation the impedance was set to match a SCR of 3 and 4 in the two cases respectively. This is considered as the buses being strong with low risk of any instability. As the series compensation increases the system impedance decreases and this results in the SCR increasing. Series compensation was varioed among 0, 5, 10, 15, and 25 % series compensation of the line.

3.1.3 SCR in Multi Converter System

The cases considered thus far have involved only a single converter connected to a passive grid. In practice, however, multiple CBRs with varying control strategies and technologies are typically present in the surrounding system. As the number of CBRs in the grid increases, the challenges associated with stability analysis are compounded, further limiting the applicability of simplified screening methods.

To enable a more tractable evaluation of the collective influence of multiple CBRs on system strength, the configuration shown in Figure 3.3 was simulated in PSCAD. This case includes three wind farms based on the type 4 wind turbine model described in Section 3.1.1. Each wind farm is connected to a bus with a SCR = 3, which is well above the threshold previously identified for stable operation of a single wind farm. The results of this analysis are presented in Section 4.1.3.

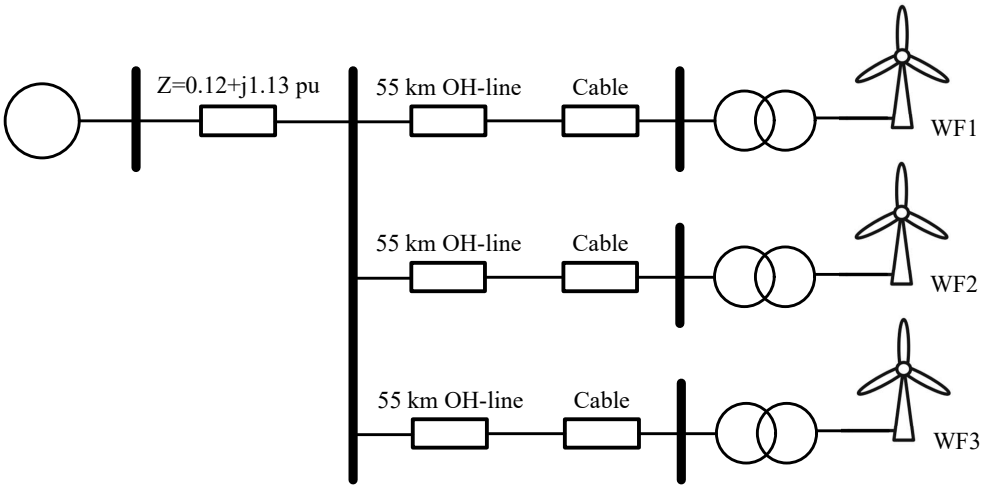

Figure 3.3: System with 3 equivalent branches

3.2 Overview and Selection of Alternative System Strength Metrics

A wide range of screening metrics are available for evaluating system strength and various aspects of system stability, as discussed in Section 2.5, 2.6 and 2.8. The initial study of alternative system strength metrics aimed to build a base level of understanding of these metrics and, based on this evaluation, select alternative metrics for further analysis. This section outlines how the preliminary small-scale case studies were performed and the rationale behind the selection of alternative metrics for more detailed evaluation.

3.2.1 Case Studies: Models

The case studies was conducted using data from PSS®E to calculate the metrics and PSCAD to assess stability. Eight distinct cases were defined, each derived from variations of two base systems. The first system comprise five distinct cases featuring varying network topologies. This setup enables a customizable network configuration, allowing different line segments to be interconnected and the electrical distance between two CBRs to be adjusted. The second system is designed to investigate the effects of increasing the number of CBRs while maintaining a fixed system configuration. The configurations for the first three cases of the first system are illustrated in Figure 3.4.

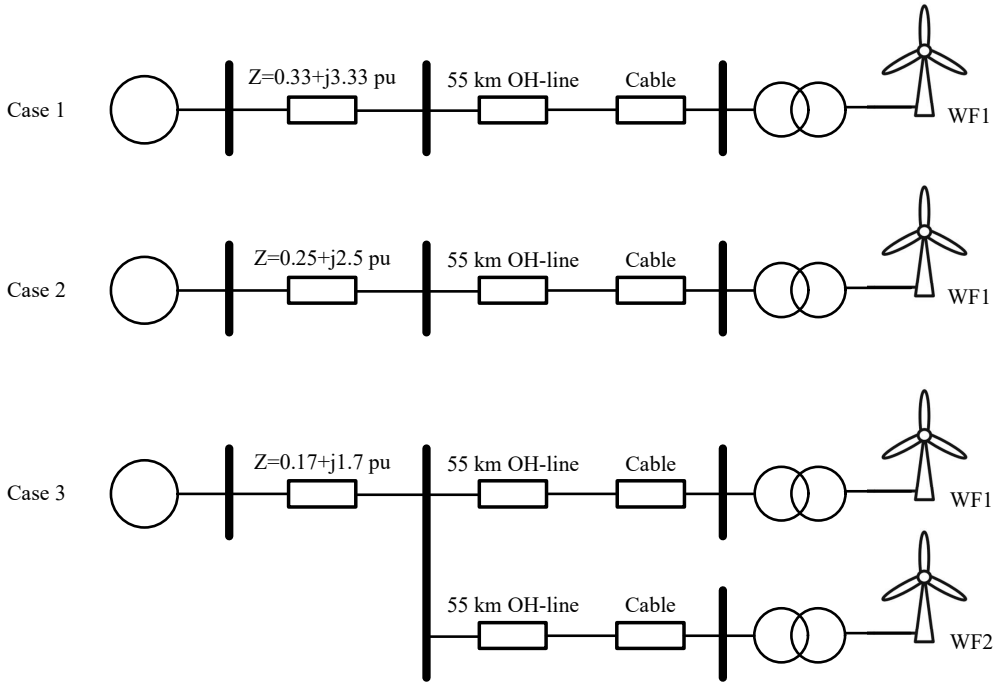

Figure 3.4: Case 1-3

The cases shown in Figure 3.4 are defined as follows:

- Case 1: the wind farm, WF1, is connected to the system via a transformer, cable, OH-line and impedance Z.
- Case 2: Same as Case 1, but impedance Z is changed. At steady state WF1 provides 200 MW and 16.5 Mvar.
- Case 3: an identical branch is connected in parallel to the first. The impedance is reduced and WF1 and WF2 both provide 200 MW and 37.3 Mvar.
- Case 3 alt2: For alternate operation WF1 provide 200 MW, 25.2 Mvar. WF2 provides the same reactive output in 25.2 Mvar but has reduced active power at 170 MW.

Cases 4 and 5, illustrated in Figure 3.5, investigate the effect of increasing electrical distance between CBRs.

- Case 4: the network topology and the impedance are changed to increase the electrical distance between WF1 and WF2. WF1 supplies 200 MW and 2 Mvar and WF2 supplies 200 MW and 23 Mvar.
- Case 5: the network topology is changed to further separate WF1 and WF2 electrically and the impedance is increased further. WF1 and WF2 both provide 200 MW and 16.5 Mvar

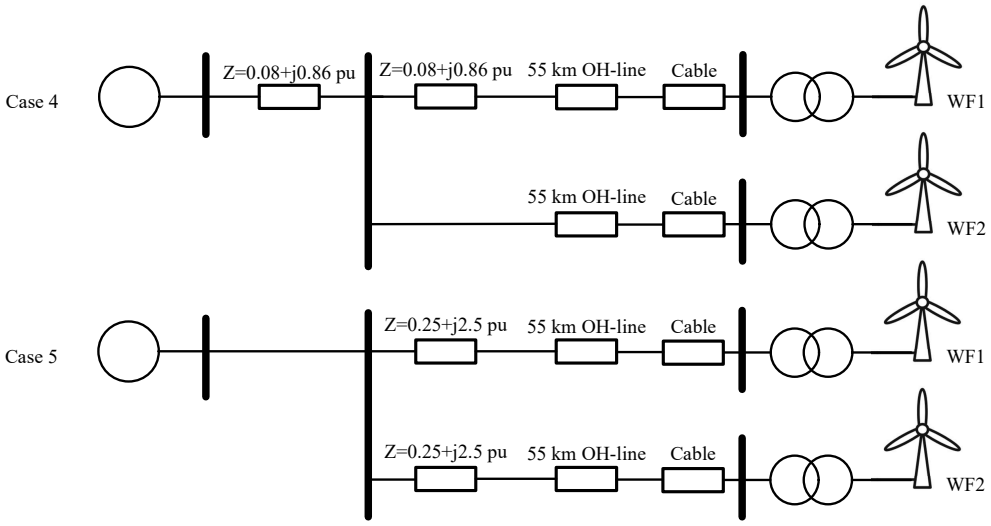

Figure 3.5: Case 5 and 6 with changing electrical distance

The second system, used to examine the effect of increasing converter-based generation, is based on the layout shown in Figure 3.3 in Section 3.1.3. Here, three additional cases were defined by incrementally increasing the number of connected wind farms.

- Case 6: WF1 has an output of 200 MW and -48 Mvar, no output from WF2, WF3.
- Case 7: WF1 and WF2 have an output of 200 MW and 0 Mvar, no output from WF3.
- Case 8: All three wind farms have an output of 200 MW and 30 Mvar

3.2.2 Evaluated Metrics

A comprehensive evaluation of all system strength metrics presented in Section 2.5, 2.6 and 2.8 could not be conducted across the full set of case studies. Instead, a subset of metrics was chosen for further assessment. The SCR was included as a reference metric representative off traditional system strength. Among the metrics,

WSCR, CSCR, EqSCR, SDSCR, and AFL were identified as sufficiently relevant for the initial analysis. In contrast, ESCR, MIESCR, and ISCR were not considered to offer additional insights compared to their respective simpler counterparts. This decision was based on the comparison between SCR and ESCR discussed in Section 2.6.5, which suggested limited added value from the extended formulations.

Furthermore, the interaction factor methods, UIF, CMIIF, EMIIF and RF were evaluated. While these metrics are not able to provide an estimation of system strength on their own, their evaluation can provide valuable insight for SCR-based measurements that utilize them. Therefore, the unweighted simple MIIF and the impedance-based interaction factor in SDSCR were evaluated as well.

3.3 Evaluation and Verification of Alternative System Strength Metrics

This section presents the evaluation and verification of alternative metrics that were selected based on the initial investigation in Section 3.2. The section begins by describing the base model developed to assess the alternative metrics in a converter-dominated power system. It then continues with the evaluation of alternative metrics, which focuses on two aspects: the accuracy of each metric in classifying system strength, and the ability of each metric to predict weak system conditions that are at risk of system instability.

To enable an automated metric calculation, Python scripts were developed using functions from the PSS®E API. These scripts are based on the metric definitions presented in Chapter 2 and are included in Appendices B.1–B.3.

3.3.1 PSSE Base Model

The base model in PSS®E was developed internally at SVK to provide a realistic representation of the Swedish power system with a high penetration of CBRs. The simplified Single-Line Diagram (SLD) of the model is presented in Figure 3.6, and a more detailed breakdown of the components is available in Appendix A.

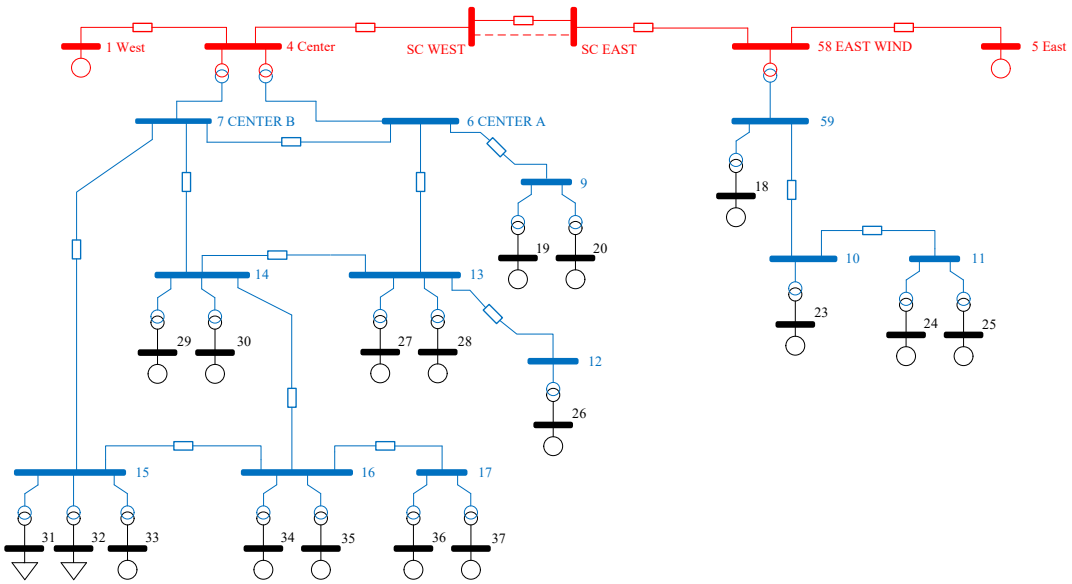

Figure 3.6: Simplified SLD of the base model used for verification of system strength metrics

The red segment in the SLD represents the 400 kV grid, which corresponds to the transmission level in the Swedish power system. In this model the slack bus is located at bus 1 and two transformer substations are located at bus 4 and bus 58, respectively. The generators at bus 5 and bus 1 are modeled as a Thévenin equivalent to represent of the power system beyond these points. One notable addition is the OH-line between bus 4 and bus 58, which is series-compensated to 50 %.

The blue segments of the SLD represent the 135 kV level, which corresponds to the sub-transmission level of the power system. Notably buses 6 and 7 are connected by a zero-impedance line to unify them as a single station. The black segments represent the 33 kV level, which represents the MV-collection grid within a wind farm and the park transformer that connects it to the sub-transmission network.

The individual wind turbines and turbine transformers, which constitute a wind farm, are aggregated as a single machine element in PSS®E. A total of 16 wind farms of Type 3 and Type 4 have been connected at the MV-level. In Table 3.3the size and type of each wind farm in the grid is presented, with the turbines connected to Station 58 East Wind presented in the top two rows, followed by those connected to 4 Center below.

Table 3.3: Bus, type and active power wind farms in base model

Bus	Type	P_{gen} [MW]	Bus	Type	P*gen* [MW]
18	Type 3	80 MW	23	Type 4	75 MW
24	Type 4	80 MW	25	Type 4	80 MW
19	Type 4	80 MW	20	Type 4	80 MW
26	Type 3	80 MW	27	Type 3	100 MW
28	Type 3	95 MW	29	Type 3	95 MW
30	Type 3	95 MW	33	Type 4	95 MW
34	Type 4	70 MW	34	Type 4	70 MW
35	Type 3	70 MW	36	Type 3	70 MW

The cable networks which normally constitute the collection grid before connecting to the park transformer are replaced and instead modeled as a capacitive shunts at each CBR-bus, ranging in size between 1-5 Mvar.

3.3.2 Verification of Estimated Strength

To verify the accuracy of the alternative metrics in estimating system strength, the base model introduced in Section 3.3.1 was used. The system strength at selected buses was estimated using the alternative metrics. An exact copy of the model in PSS®E was then converted to PSCAD for the simulation of the dynamic response. This meant that the different CBRs in PSS®E were modeled using the PSCAD simulation models for Type 3 and 4 wind turbines described in Sections 3.1.2 and 3.1.1, respectively. The verification of the estimated system strength obtained from the alternative metrics was achieved by introducing a 100 ms voltage dip of 5 % at buses with different system strength. The response to this perturbation was then studied for the different buses. Since traditional system strength is closely correlated with voltage stiffness, buses with higher estimated strength are expected to recover to pre-disturbance conditions faster than weaker buses.

3.3.3 Prediction of Weak System Conditions Using Alternative Metrics

The investigation of the accuracy of the alternative metrics in predicting weak system conditions was performed across multiple system configurations. For each case, the output of the wind farm was gradually increased. Subsequently, the system strength metrics were calculated for each case and corresponding PSCAD simulations were performed at each level of increased power output to determine the point at which the system became unstable. By comparing the PSCAD stability results with PSS®E metric calculations, the accuracy of each metric in predicting weak system conditions and instabilities could be evaluated.

All cases were adaptations of the base model presented in Section 3.3.1, including corresponding EMT models to enable detailed stability analysis. These cases differ in both system topology and the number of connected CBRs, allowing an evaluation of metric performance under changing CBR penetration levels. The six defined cases are:

- **Case A**: The base model as presented in Section 3.3.1.
- **Case B**: Disconnected the 400 kV system at bus 5, and the series compensation on the overhead line between buses 4 and 58 was bypassed.
- **Case C**: The zero-impedance line between buses A and B at the central 400/135 kV station and the overhead line between buses 13 and 14 were disconnected, effectively splitting the center station into two smaller stations and altering CBR interactions.
- **Case D**: The maximum number of wind farms connected to each 135 kV bus was limited to one by disconnecting wind farms 20, 25, 28, 30, 35, and 37.
- **Case E**: All but eight wind farms were disconnected (wind farms 18, 19, 23, 27, 29, 33, 34, and 36 remained connected).
- **Case F**: All but four wind farms were disconnected (wind farms 19, 29, 33, and 36 remained connected).

4

Results and Analysis

This chapter presents the results of the initial evaluation of traditional system strength estimation, the initial evaluation of alternative system strength metrics and the final evaluation and verification using PSS®E and PSCAD.

4.1 Evaluation of Traditional System Strength

This section presents the results of the initial study of traditional system strength estimation using SCR outlined in Section 3.1

4.1.1 SCR in Single Converter System

The simulation described in Section 3.1.1 found that, for defined case, the minimum SCR value for stable operation is 1.4. This observation is shown in Figure 4.1, which illustrates the Root Mean Square (RMS) voltage at the wind farm. During the startup sequence, the SCR is set to 1.4 and the wind farm is then stabilized at full power. The steady state condition is shown in Figure 4.1 for the interval between 0-0.2 s at the beginning of the simulation. At T=0.2 s the SCR is changed to 1.3; as can be seen, the system becomes unstable with evident oscillation in the RMS voltage. The oscillation in the RMS voltage has a frequency of 5 Hz, which can be compared with the results of an impedance-based analysis. Note that the wind farm is injecting 67.5 Mvar reactive power in this case which is lower than the wind farm rated reactive power.

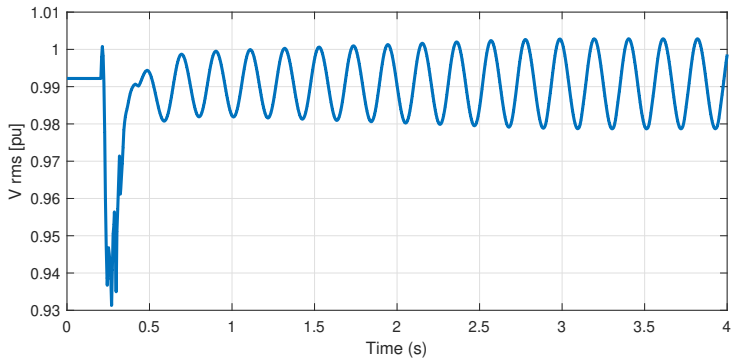

Figure 4.1: RMS voltage at wind farm

The result of the admittance scan for a system with SCR values of 1.4 and 1.3

are presented in Figure 4.2 and 4.3. From the figures, it can be noted how the magnitude of the grid impedance intersects the converter impedance magnitude in two areas, around 45 and 55 Hz in the SCR=1.3 case. This corresponds to the 5 Hz oscillations that were observed for the RMS voltage in Figure 4.1. The impedance curve of the converter exhibits negative phase angles in these regions, indicating its capacitive nature. Conversely, the grid demonstrates a positive phase angle, reflecting its inductive characteristics. This configuration results in resonances at the intersection points of these impedance curves. The significant phase differences of 211 and 185° at these intersections signify negative damping, which leads to the instability observed in the RMS voltage of the wind farm, as illustrated in Figure 4.1[1]. When the SCR is increased to 1.4, the impedance curves no longer intersect, corroborating the stable operation observed in the simulation study under these conditions.

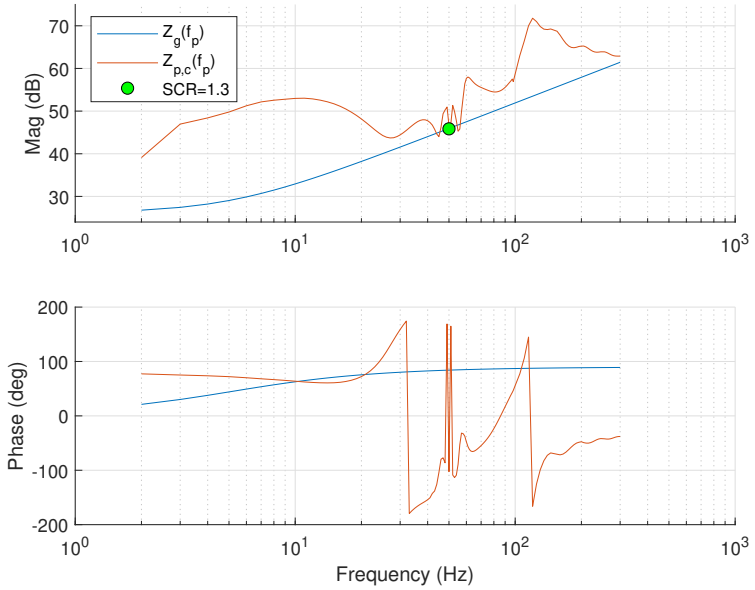

Figure 4.2: Bode-diagram of $Z_{p,c}(f_p)$ and $Z_g(f_p)$ with SCR=1.3

[1]As noted in section 2.5 an analysis of the Nyquist diagram is needed for a complete stability study. This was not performed in this case since it was complimented by EMT simulations.

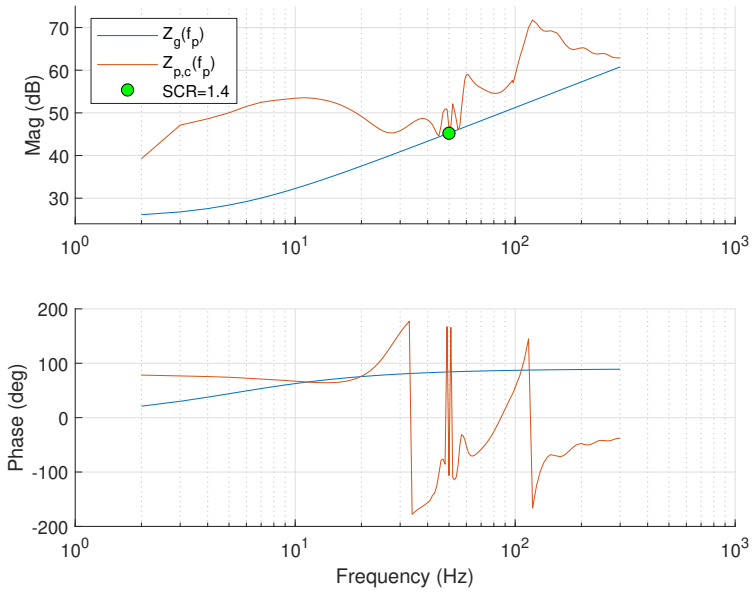

Figure 4.3: Bode-diagram of $Z_{p,c}(f_p)$ and $Z_g(f_p)$ with SCR=1.4

Equation (2.7) in Section 2.3.1 demonstrates how SCR is closely tied to system impedance at 50 Hz. In Figure 4.3 and 4.2 this relationship has been used to calculate the Thévenin impedance from the SCR. This is marked by the green dot in the figures and it can be seen how these points match with the grid impedance curve at 50 Hz in Figures 4.2 and 4.3. In a traditional power system where the system impedance is approximated to an RL curve this point can provide an estimation of the overall magnitude of the impedance curve over a large frequency spectrum. A lower SCR corresponds to a generally higher magnitude of the system impedance curve, which in turn increases the likelihood of an intersection between the grid and converter impedance curves. This relationship explains why SCR is often considered a relatively effective metric for assessing grid strength, particularly in the context of single CBR connections. For instance, a grid with an SCR greater than 3 is significantly less prone to such intersections compared to systems with SCR values of 2 or 1.

However, if the control design is suboptimal-such as when employing an excessively fast PLL or AC voltage controls that are not well-coordinated with the overall control strategy, the impedance curve of the CBR may shift [35]. This increases the risk of intersection even at SCR values higher than 1.3 and at frequencies other than 45 or 55 Hz. The grid example used in this case study is also oversimplified to an RL circuit. However, a realistic grid impedance is not linear. In the presence of capacitance from cables, series compensation, and other CBRs in the grid, the grid impedance exhibits series or parallel resonances, which increase the chance of intersections between these two impedances at a broader frequency range around the fundamental. There are several other factors that impact the SCR threshold of instability, such as grid X/R ratio, loads, shunt compensators, etc. Consequently, SCR cannot provide a definitive assessment of system stability or establish a universally reliable threshold.

4.1.2 SCR in Series Compensated System

Simulations were conducted for a Type 3 wind farm connected according to the two models presented in 3.1.2, with the results presented in table 4.1

Table 4.1: Simulation of Type 3 wind farm with radial series compensated connection and parallel connection

	System conditions	Radial	Parallel
SCR=3	SC=0%	Stable	Stable
	SC=5%	Unstable	Stable
	SC=10%	Unstable	Unstable
	SC=15%	Unstable	Unstable
	SC=25%	Unstable	Unstable
SCR=4	SC=0%	Stable	Stable
	SC=5%	Unstable	Stable
	SC=10%	Unstable	Stable
	SC=15%	Unstable	Stable
	SC=25%	Unstable	Stable

It can be observed, how the wind farm with a purely radial connection becomes unstable for lower levels of series compensation, regardless of SCR estimating the bus as strong. With a parallel line connected, the issue is significantly less pronounced. While Type 3 wind turbines are considered particularly sensitive to series compensation, this affects Type 4 wind turbines as well. Furthermore, this is a phenomenon occurring in the subsynchronous frequency range, and therefore SCR is unable to detect the impact of such conditions on system strength.

4.1.3 SCR in Multi Converter System

The results of the simulation described in Section 3.1.3 show how the aggregate impact of multiple wind farms can cause the system to become unstable, even though each of the individual connections id above the threshold at which the bus is considered strong according to the SCR. This is illustrated in Figure 4.4 where the POC voltage and generated active power are plotted.

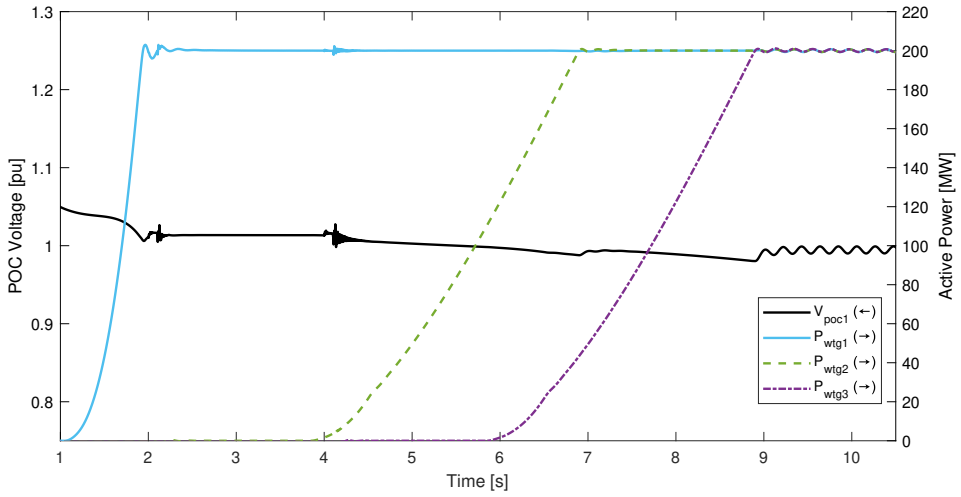

Figure 4.4: POC voltage and active power for staggered activation of 3 wind farms

As can be seen in Figure 4.4, the start of each wind farm is staggered. When the third wind farm is connected and increases it´s power output, the voltage starts to oscillate. This demonstrates that as the amount of CBR production increases, the estimation of system strength using SCR fails to account for the potential interaction between multiple converters.

The impedance-based stability analysis or other alternative screening metrics explained previously can be used to capture such instabilities in a multi-converter system. However, the impedance-based method requires the converter impedances to be known, which are usually unknown in the grid planning stage. Consequently, it is difficult to use impedance-based methods for grid strength assessment in an early grid planning stage for integration of CBRs in the grid, which is why this method is outside the scope of this work.

4.2 Overview and Selection of Alternative System Strength Metrics

This section presents the results of small-scale case studies performed for an initial evaluation of interaction factors and SCR-based system strength metrics and the selection of alternative system strength metrics for further detailed evaluation.

4.2.1 Case studies

The results of the interaction factors and SCR-based system strength metrics for the eight cases presented in Section 3.2 are compiled in Tables 4.2 and 4.3, respectively.

Interaction factors

Table 4.2 summarizes the results for the tested interaction factors, including both the unweighted amplitude- and angle-based MIIF, as well as the impedance-based interaction factor used by SDSCR. Results are not provided for cases 1, 2, and 6, as these cases include only a single CBR, and interaction factors can only assess risk of interaction between multiple CBRs. Furthermore, results for the third wind farm in case 8 are omitted due to the symmetrical nature of the case, which leads to identical interaction factors for wind farm 3 as for the interactions between wind farms 1 and 2. The results fall in the range between 0 and 1, where 0 indicates the CBRs are electrically distant with no interaction and 1 indicates they can be assumed to be connected at the same point with full interaction. Therefore as the value of interaction factor increases, the risk of interaction between the two CBRs also increases.

Table 4.2: Interaction factor results from case studies

		Case 3 Unstable	Case 3 alt 2 Stable	Case 4 Stable	Case 5 Stable	Case 7 Stable	Case 8 Unstable
Wind farm 1	UIF_{21}	0.58	0.69	0.44	0	0.52	0.52
	$MIIF_{21,amp}$	0.81	0.81	0.67	0	0.75	0.75
	$CMIIF_{w,21,amp}$	0.81	0.97	0.67	0	0.75	0.75
	$EMIIF_{w,21,amp}$	0.81	0.97	0.67	0	0.75	0.75
	$MIIF_{21,ang}$	0.82	0.82	0.67	0	0.75	0.75
	$EMIIF_{w,21,ang}$	0.82	0.97	0.68	0	0.75	0.75
	IF_{21}(SDSCR)	0.76	0.76	0.66	0	0.71	0.71
	RF_{21}	0.76	0.76	0.49	0	0.71	0.71
Wind farm 2	UIF_{12}	0.58	0.50	0.15	0	0.52	0.52
	$MIIF_{12,amp}$	0.81	0.81	0.42	0	0.75	0.75
	$CMIIF_{w,12,amp}$	0.81	0.7	0.42	0	0.75	0.75
	$EMIIF_{w,12,amp}$	0.81	0.69	0.42	0	0.75	0.75
	$MIIF_{12,ang}$	0.82	0.69	0.41	0	0.75	0.75
	$EMIIF_{w,12,ang}$	0.82	0.82	0.41	0	0.75	0.75
	IF_{12} (SDSCR)	0.76	0.76	0.39	0	0.71	0.71
	RF_{12}	0.76	0.76	0.49	0	0.71	0.71

Several observations can be made from the results presented in Table 4.2. First, all measurements indicate a relatively high risk of interaction for all cases except Case 5, in which the wind farms are electrically the most separated due to the system configuration. Additionally, the in-ability to account for the effects of multiple CBRs can be observed, which is well illustrated in Cases 7 and 8. In Case 8, only two CBRs are connected, and although the estimated risk of interaction is high, the system remains stable. However, in case 8, the addition of a third CBR results in an aggregated interaction that leads to system instability, even though the interaction estimation between each wind farm remains the same. As discussed in Section 2.8, interaction factors are designed to capture interactions between two CBRs and may not provide a complete measure of overall system strength. However, valuable

insights can still be gained from examining the performance of individual interaction factors to gain a greater understanding of the differences between SCR-based metrics.

Looking at individual metrics, the UIF provides the least conservative estimation of system strength, yielding the lowest estimated risk of interaction. Another aspect captured by UIF is the influence of CBR size on the estimated risk. As shown in equation (2.31), changes in power affect the UIF, which can be observed when comparing Case 3 and Case 3 alt 2. In these cases, the system configuration remains unchanged but the power ratings of the CBRs differ.

The results for amplitude- and angle-based MIIF are noteworthy. The unweighted MIIF provides the least conservative estimates, indicating the highest interaction risk. The close similarity between amplitude- and angle-based MIIF suggests that, at least for these small-scale systems, they yield comparable results.

Withe respect to the weighted variants of MIIF, there are few cases demonstrating the impact of CMIIF and EMIIF. This is due to most scenarios involving CBRs of equal size, resulting in a weighting factor of 1. However, Case 3 highlights the effect of weighting when wind farm 2 is smaller. Both weighted CMIIF and EMIIF demonstrate that the larger wind farm 1 exerts a greater influence on wind farm 2, whereas this is not reflected in the unweighted versions, which do not account for rated active or reactive power.

The impedance-based interaction factor used in SDSCR tends to yield slightly less conservative estimates compared to the unweighted MIIF applied by EqSCR. This is expected, as they are inherently similar, yet it explains the differences observed later in the SCR-based measurements. Overall, the interaction factor results align with other unweighted interaction factors, which do not consider the relative size of the CBRs.

Finally, the RF interaction factor for 50 Hz considers only electrical distance, which is evident in its results remaining unchanged between case 3 and case 3 alt 2. Generally, it estimates interaction at 50 Hz and is slightly less conservative than the unweighted MIIF.

Overall, the small-scale study of interaction factors confirmed that they only consider interaction between two CBRs at a time. This means they are unable to provide an overall estimation of system strength that accounts for multiple CBRs at simultaneously. instead, they offer an estimation of risk for interaction which can have an adverse effect on system strength. The interaction factor that provided the most conservative overall estimation for risk of interaction risk was MIIF, which is already utilized in EqSCR. The impedance-based interaction factor utilized by SDSCR shares fundamental similarities but provides a slightly less conservative estimation of interaction due to the differences in calculation methods.

SCR-based metrics

The results for the IFs in the case studies help in understanding some of the SCR-based metrics, such as EqSCR and SDSCR. Table 4.3 presents the results for the four alternative SCR-based metrics, the AFL applied with two different MSCRs, and the SCR as a reference point.

Table 4.3: Summary results from case studies for AFL and SCR-based metrics

		Case 1 Unstable	Case 2 Stable	Case 3 Unstable	Case 3 alt 2 Stable	Case 4 Stable	Case 5 Stable	Case 6 Stable	Case 7 Stable	Case 8 Unstable
Wind farm 1	SCR	1.2	1.6	2.2	2.2	2.2	1.6	3.1	3.0	3,0
	WSCR	1.2	1.6	0.9	1.1	1.48	0.8	3.1	1.5	1.0
	CSCR	1.2	1.6	1.2	1.3	2.0	1.57	3.1	1.73	1.18
	EqSCR	1.2	1.6	1.21	1.30	1.56	1.6	3.1	1.74	1.18
	SDSCR	1.2	1.6	1.2	1.32	1.6	1.6	3.1	1.8	1.2
	AFL(1.6)	-80	0	-50	-30	80	0	270	120	0
	AFL(2)	-160	-80	-160	-140	0	-80	190	20	-130
Wind farm 2	SCR	N/A	N/A	2.2	2.59	3.7	1.6	N/A	3.0	3.0
	WSCR	N/A	N/A	0.9	1.1	1.48	0.8	N/A	1.5	1.0
	CSCR	N/A	N/A	1.2	1.3	2.0	1.57	N/A	1.73	1.18
	EqSCR	N/A	N/A	1.21	1.32	2.21	1.6	N/A	1.74	1.18
	SDSCR	N/A	N/A	1.2	1.35	2.36	1.6	N/A	1.8	1.2
	AFL(1.6)	N/A	N/A	-50	0	310	0	N/A	120	0
	AFL(2)	N/A	N/A	-160	-100	220	-80	N/A	20	-130
Wind farm 3	SCR	N/A	N/A	N/A	N/A	N/A	N/A	N/A	N/A	3.0
	WSCR	N/A	N/A	N/A	N/A	N/A	N/A	N/A	N/A	1.0
	CSCR	N/A	N/A	N/A	N/A	N/A	N/A	N/A	N/A	1.18
	EqSCR	N/A	N/A	N/A	N/A	N/A	N/A	N/A	N/A	1.18
	SDSCR	N/A	N/A	N/A	N/A	N/A	N/A	N/A	N/A	1.2
	AFL(1.6)	N/A	N/A	N/A	N/A	N/A	N/A	N/A	N/A	-130
	AFL(2)	N/A	N/A	N/A	N/A	N/A	N/A	N/A	N/A	0

The results for SCR presented in Table 4.3 illustrate two aspects of system strength estimation with which SCR struggles in systems featuring a high penetration of CBRs. These are mainly the overestimation of system strength and the inability to accounting for changes in the surrounding system. The overestimation is clearly demonstrated by Cases 6-8, where the increase in CBRs from case to case eventually leads to system instability in Case 8, despite the SCR for all wind farms in Case 6-8 remaining the same. SCR's response to different system conditions can be seen by comparing Case 3 and Case 3 alt 2. The SCR of wind farm 1 remains unchanged, but a reduced rated power of wind farm 2 increases system strength. This increase is not reflected in the system strength estimation for wind farm 1.

The results of WSCR in Table 4.3 illustrate both its strengths and weaknesses. WSCR provides a better estimation of system strength when the number of CBRs change as seen from Case 6 to Case 8. However, WSCR is not suitable in cases where the CBRs cannot be considered electrically close to each other. This is evident in the outcome that WSCR=0.8 for Case 5, where the system is stable, while

WSCR=0.9 for Case 3, where the system is unstable. This discrepancy arises due to the assumption of full interaction in the WSCR calculation. When the electrical distance is altered, a case-by-case consideration is necessary to determine which CBRs should be included in the calculation.

CSCR provides a less conservative estimation of system strength compered to WSCR. In cases with a single CBR connected, it matches SCR and can consider the changing electrical distance observed in Case 4 and 5. However, similar to WSCR, CSCR provides an aggregated measurement of system strength within a limited area. This means that CSCR cannot account for the different conditions of wind farm 1 and 2 in case 4. Wind farm 1 has much lower short circuit power due to increased impedance, making it significantly weaker. Since CSCR only provides a single measurement, it is unable to identify the different strength within the group.

EqSCR and SDSCR both utilize interaction factors to scale the contribution of other CBRs through to a penalty factor. For cases 1 and 2, where there is a single CBR, they match the results of the traditional SCR; however, with multiple CBRs a penalty factor is introduced. The results of EqSCR and SDSCR are consistent, as the system becomes unstable when EqSCR/SDSCR is reduced below 1.3. Additionally, it is evident that as the number of CBRs increases, as in cases 6 and 7, the system strength is gradually reduced. Compared to WSCR, EqSCR and SDSCR can account for the changing electrical distances in casees 4 and 5. Whereas WSCR underestimates system strength, EqSCR/SDSCR can scale the contribution of other CBRs according to their electrical proximity.

Furthermore, the observations made by [30] are confirmed: a higher MSCR results in a more conservative measurement. This is shown by the AFL results with MSCR values of 1.6 and 2.0, respectively. Note that the results for AFL are inconsistent: use of AFL(2.0) leads to an overly conservative estimation of system strength, while AFL(1.6) provides a better estimation, but it overestimates system strength for case 8, which EMT simulations indicated to be unstable.

4.2.2 Selection of Metrics for Further Evaluation

In the selection of alternative system strength metrics for further evaluation the interaction factors were excluded, as they only capture the interaction between two devices at a time. As shown in Section 4.2.1, this limitation prevents them from representing the aggregated influence of multiple surrounding CBRs. Nonetheless, they remain valuable when applied for their intended use of screening for interaction or applied in penalty factors for system strength, as done in EqSCR and SDSCR.

Of the SCR-based metrics, EqSCR and SDSCR demonstrated the most promising results for the initial case studies presented in Section 4.2.1. In particular, EqSCR and SDSCR were able to provide consistent estimation of instability for different cases and to take into account the variations in electrical separation between CBRs. EqSCR and SDSCR also provide individual measurements for each bus, which means

that the weakest point of the system can be identified while taking other CBRs in to account.

WSCR was not considered suitable due to its underlying assumption of full interaction between all CBRs within the aggregated measurement. While this approach may be useful under specific conditions, it tends to underestimate system strength in more complex system configurations. Additionally, it provides a measurement for a group which means that WSCR can not be utilized for identifying the weakest CBR in the system. While CSCR produced more consistent results compared to WSCR, it too can only provide a single aggregated value for a group of CBRs. This is since it is aimed at aggregating system strength for CBRs within a wind farm. However, this means that CSCR, similar to WSCR, cannot identify which single CBR is the weak point - something which can be valuable when planning the future power system.

The final evaluated metric, AFL, has some beneficial characteristics, since it not only provides an estimate of system stability but it also offers a straightforward method for determining the maximum allowable capacity of a new plant. This feature is particularly beneficial during early-stage screening, when system operators may need to assess the feasibility of new converter-based plants at specific connection points. However, as shown in Section 4.2.1, AFL's performance is sensitive to the choice of MSCR. Minor changes in MSCR significantly affect the AFL results and thus can result in an unnecessarily high number of detailed EMT studies. Additionally, AFL(1.6) showed limitations under high CBR penetration. While it performed well for two-CBR scenarios, it overestimated system strength in Case 8.

Despite these limitations, AFL was deemed to have sufficient potential to warrant further evaluation. A detailed evaluation may help to determine its viability as a screening tool for system strength in large-scale applications. Thus, the three metrics selected for further evaluation were EqSCR, SDSCR, and AFL.

4.3 Evaluation and Verification of Alternative System Strength Metrics

This section presents the results of the evaluation of AFL, EqSCR and SDSCR using PSS®E and PSCAD based on the approach presented in Section 3.3.

4.3.1 Verification of Estimated Strength

To verify AFL, EqSCR and SDSCR, these metrics were calculated for the base model presented in Section 3.3.1 as well as for the base model with generated power scaled by 110 %. The results for the estimation of system strength are presented in Table 4.4.

Table 4.4: Calculated system strength for Base model and Base model x 1.1

			Base model				Base model x 1.1			
Bus	Type	SC_i	SCR	AFL	EqSCR	SDSCR	SCR	AFL	EqSCR	SDSCR
18	Type 3	530	6.6	271.0	2.75	2.79	6.0	246.0	2.5	2.54
19	Type 4	553	6.9	351.0	2.06	2.12	6.3	333.0	1.87	1.93
20	Type 4	553	6.9	351.0	2.06	2.12	6.3	333.0	1.87	1.93
23	Type 4	508	6.8	293.0	2.22	2.27	6.2	274.0	2.02	2.06
24	Type 4	462	5.8	237.0	2.05	2.1	5.2	217.0	1.87	1.9
25	Type 4	462	5.8	237.0	2.05	2.1	5.2	217.0	1.87	1.91
26	Type 3	500	6.2	213.0	1.8	1.86	5.7	187.0	1.63	1.69
27	Type 3	682	6.8	298.0	1.9	1.96	6.2	263.0	1.72	1.78
28	Type 3	680	7.2	310.0	1.91	1.98	6.5	278.0	1.74	1.8
29	Type 3	694	7.3	322.0	1.92	1.98	6.6	290.0	1.74	1.8
30	Type 3	695	7.3	324.0	1.92	1.98	6.7	291.0	1.74	1.8
33	Type 4	590	6.2	330.0	1.78	1.86	5.6	308.0	1.62	1.69
34	Type 4	481	6.9	287.0	1.71	1.79	6.2	270.0	1.56	1.62
35	Type 4	481	6.9	287.0	1.71	1.79	6.2	270.0	1.56	1.62
36	Type 3	425	6.1	165.0	1.6	1.67	5.5	141.0	1.45	1.52
37	Type 3	425	6.1	165.0	1.6	1.67	5.5	142.0	1.45	1.52
			Stable				Stable			

According to the results for EqSCR and SDSCR, the weakest points in the system are buses 36 and 37, with an EqSCR=1.6 and SDSCR=1.67. At these buses, Type 3 wind farms are connected. The strongest point in the system is bus 18, with EqSCR=2.75 and SDSCR=2.79. Similar to buses 36 and 37, a Type 3 wind farm is also connected at bus 18. The results for SCR show a similar trend when considering the strength of buses 18 and 36/37, with the stronger bus having SCR=6.6 and the weaker bus SCR=6.1, which suggests a difference in system strength. The results are also similar for AFL, with bus 18 considered much stronger than buses 36/37.

In Section 2.3, system strength was defined as the ability to withstand voltage deviations in response to changes in current. To illustrate this strength, EMT simulations are conducted in PSCAD, providing a qualitative demonstration of system strength. The objective is to apply a voltage perturbation and observe the resulting impact on voltage and power output. It is expected that a stronger point will exhibit fewer oscillations and faster recovery after the perturbations. In Figure 4.5, the voltage and active power are plotted for buses 18 and 36 when a perturbation, in form of a 5 % voltage drop, is introduced. Figure 4.5 also present the system response for the base model and the base model operated at 110 % power.

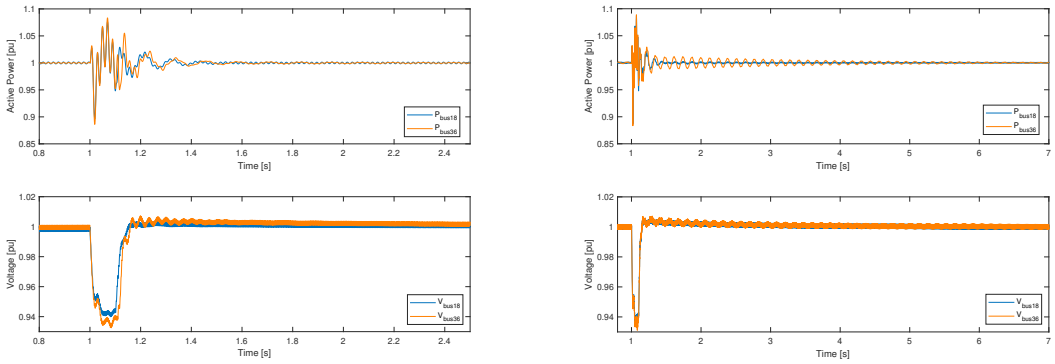

(a) Base model **(b)** Base model x 1.1

Figure 4.5: Response of bus 18 and 36 to a 5 % voltage dip the respective bus

Figure 4.5a shows how the initial response to the voltage dip for buses 18 and 36 is similar. However, it is clear that bus 18 recovers more quickly after the voltage dip, exhibiting fewer voltage oscillations compered to bus 36. This is consistent with how the alternative metrics have estimated system strength for the two buses. The same dynamic behavior is observed in the simulation with increased generated power. As seen in Table 4.4, the estimated system strength is reduced for buses 18 and 36. Observing the simulation results in Figure 4.5b, it is clear that the voltage oscillations at bus 36 persist much longer compared to the simulation of the base model. This indicates that the system strength has been reduced and supports the change in system strength shown by the calculation of the SCR as well as by the alternative system strength metrics.

Thus far, the analysis has focused solely on buses with Type 3 turbines; however, a comparable analysis was performed for the strongest and weakest points where a Type 4 wind farm is connected. According to the results presented in Table 4.4, bus 23 is the strongest bus with EqSCR= 2.22 and SDSCR= 2.27, and buses 34/35 are the weakest with EqSCR=1.71, SDSCR= 1.79. The results for SCR and AFL, on the other hand, are nearly identical for the two buses, with SCR=6.8, AFL=293 for bus 23 and SCR=6.9, AFL=287 for buses 34/35. This indicates a similar system strength for both buses according to these metrics. The simulation results for the introduced voltage dip are presented in Figure 4.6.

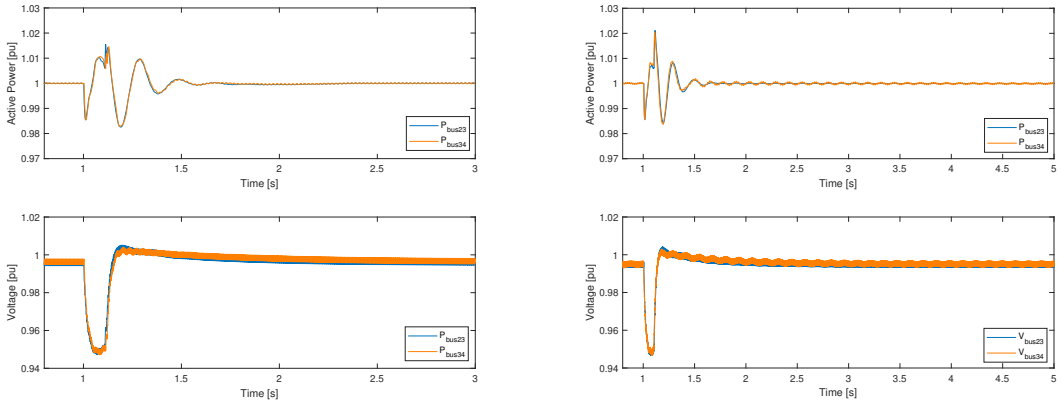

(a) Base model **(b)** Base model x 1.1

Figure 4.6: Response of bus 23 and 34 to a 5 % voltage dip the respective bus

In Figure 4.6a, limited voltage oscillations are observed at bus 34, which are not present at bus 23. This suggests a difference in system strength, as reflected by the EqSCR and SDSCR indices. The trend becomes more pronounced under weaker system conditions. As shown in Figure 4.6b, the voltage recovery time at bus 34 is significantly longer, with oscillations also present in the voltage waveform at bus 34. This indicates that EqSCR and SDSCR provide a more accurate estimation of system strength compared to traditional SCR and AFL, which indicate similar strength levels for buses 34 and 23, highlighting their limitations in this context.

These simulations demonstrate that EqSCR and SDSCR provide a better estimation of system strength compared to SCR and AFL. Additionally, it appeares that the PSCAD model used for Type 4 wind farms used in this project is more capable to withstand low system strength than the Type 3 wind farm. However, this is model specific, and as previously discussed in Section 2.4, different control parameters can have a significant impact on the behavior and stability of a wind turbine. Therefore, it is plausible the implementation of voltage control in the Type 3 model contributes to its lower tolerance for interaction.

4.3.2 Prediction of Weak System Conditions Using Alternative System Strength Metrics

The complete results for all metrics across all buses under varying generation levels are available in Appendix C, Tables C.1–C.6.To summarize these results, the weakest bus was identified as the one with the lowest metric value, which was used as an indicator of overall system vulnerability. Table 4.5 presents the aggregated results of the lowest value for each metric at the generation level at which instability first occurs for each of the six evaluated cases.

Table 4.5: Aggregated results, case A-B, for weakest bus when system becomes unstable

Case	SCR	AFL	EqSCR	SDSCR
A x 1.3	4.4	95	1.20	1.29
B x 1.1	4.5	92	1.06	1.12
C x 1.3	4.2	52	1.18	1.26
D x 2.0	2.9	-32	1.20	1.26
E x 2.2	2.8	-73	1.20	1.26
F x 2.8	2.2	-188	1.27	1.33

Traditionally, SCR thresholds at the MV-bus categorize system strength as follows: values above 4 indicate a very strong system; values between 4 and 2 suggest decreasing strength; and values below 2 indicate a very weak system. SDSCR uses the same thresholds, as referenced in [25], while EqSCR applies a threshold of 2 for screening system strength [36]. AFL, based on different principles, considers negative values as indicative of weak system strength [8].

Applying these thresholds to the results in Table 4.5, it can be noted that SCR are greater than 4 for Cases A, B, and C although the system is unstable. This corroborates with how SCR tends to overestimate system strength in cases with high CBR penetration , regardless of system configuration. Additionally, as CBR penetration decreases in Cases D-F, SCR's accuracy improves. For Casees D and E, SCR is reduced to 3, which indicate a weak system, and for Case F SCR equals 2.2, which is close to the threshold where the system could be considered very weak.

The AFL results are more challenging interpret. For Cases A–C, AFL indicates strong system strength with positive values, despite PSCAD simulations showing instability. However, as the number of CBRs is reduced in Cases D–F, AFL correlates better with instabilities observed in the EMT simulation by indicating very weak system strength with negative values. This inconsistency raises questions regarding AFL's reliability as a system strength metric in high CBR penetration contexts.

EqSCR and SDSCR demonstrate more consistent and promising results. The metrics produce nearly identical outcomes and exhibit the same trend across the different cases tested. When EqSCR falls between 1.06-1.3, the system becomes unstable, signaling very weak system strength in accordance with defined thresholds. Similarly, SDSCR values ranging from 1.12-1.33 coincide with instability- slightly less conservative than EqSCR- but still clearly indicative of a very weak system. Importantly, these results remain consistent across different system configurations and levels of CBR penetration, indicating that EqSCR and SDSCR can provide a more reliable system strength estimation in CBR-dominated systems.

An additional consideration when comparing EqSCR and SDSCR is their complexity and computation speed. Although both metrics yield similar results, they differ due

to the calculation method of the interaction factor they employ. Thus far, these metrics have primarily been applied in systems with relatively few CBRs, between 4-16. However, even with the limited cases studiese, the calculation times for EqSCR and SDSCR differed. Both metrics showedan increase in calculation time as the number of CBRs increased, but the increase was much greater for SDSCR. This suggests that, as system size and complexity grow due to an increased numbers of CBRs, the computational burden of SDSCR will raise more compared to EqSCR. Given the similarity in results, this trade-off in computational efficiency makes EqSCR the preferable choice for implementing system strength screening.

The definition of thresholds is as significant as the choice of method used to estimate system strength. Previous studies as in Cigre Technical Brochure 671 suggested the use of thresholds similar to SCR_{MV} where EqSCR below 2 is the limit where further studies are required [10]. This has been the threshold used in Fingrid's implementation of EqSCR for the purpose of slow converter driven stability and parameter tuning for CBR voltage control [36]. However, the basis for this threshold has not been clearly established. In [10] few explanations are provided for why the SCR threshold of 2 is suitable for EqSCR screening. Fingrid's report, [36], on EqSCR recognizes the need for EMT simulations to verify the results of system strength calculated using EqSCR. Although Fingrid has identified stable operation for EqSCR values lower than the critical SCR, no EMT based simulations are presented [36].

According to the results for EqSCR and stability analysis performed in this work, the following thresholds for EqSCR can be implemented.

- Strong bus: EqSCR > 2.5
- Weak bus: $2.5 >$ EqSCR > 2
- Very weak bus: EqSCR< 2

These thresholds are similar to those presented in [10] and are supported by the EMT-based simulations performed in this project. This provides a stability margin necessary to accommodate variations in operating conditions such as network topology, load and converter control parameters- all of which influence system stability. it should be noted that these effects cannot be accurately captured by SCR-based metrics. in particular, converter control parameters have been shown to impact system stability, as demonstrated by the different responses of Type 3 and Type 4 wind farms in the case studies performed.

5
Discussion

5.1 Method and Results

The concept of system strength is intended to encompass a wide range of phenomena, each of which depends on a numerous interacting factors within the power system. Due to this complexity, theoretical evaluation of each individual aspect contributing to system strength is challenging. Hence, this thesis adopts a simulation-based methodology in an EMT environment, to assess alternative system strength metrics through detailed dynamic case studies. By employing this EMT simulation approach, the aggregate impact of complex phenomena on system strength screening can be assessed.

Screening system strength inherently involves balancing accuracy against computational complexity and data availability. While impedance-based stability analysis is capable of capturing many of the emerging stability phenomena introduced by converter-dominated power systems, this project has focused on the practical needs of grid development/planning, particularly for early-stage screening of new grid connections. The screening method must therefore be able to efficiently assess a broad range of stability effects, enabling better planning and operational decisions.

SCR remains the primary tool for such screening due to its computational simplicity and particularly its low data requirements. However, as illustrated by the results in Section 4.1.1, SCR-based approaches face significant challenges when compared to detailed impedance-based studies. Any SCR-based metric is fundamentally based on quantities calculated at the fundamental system frequency (50 Hz or 60 Hz), while many of the new stability challenges associated with CBRs manifest themselves at frequencies outside this band. Traditionally, SCR has served as a proxy for system impedance, and the enhanced SCR-based alternatives incorporating interaction factors provide a more conservative estimate that considers the influence of surrounding CBRs on system stability.

Despite their improvement, EqSCR and SDSCR can not provide an exact estimation of stability in the system, since they are calculated at the fundamental frequency. Different CBRs will exhibit different behaviors for the same conditions depending on the grid conditions due to their control characteristics. EqSCR and SDSCR can not predict how a certain CBR will react to system conditions and will themselves have difficulty capturing factors outside the fundamental frequency range. This includes

factors such as variations in control parameters, PLL tuning, series compensation, and cable installations. Thus, determining stability at a certain EqSCR must be evaluated on a case-by-case basis. This is why the simulation results presented in Section 4.3.2 provide reliable estimates for the specific scenarios analyzed in this study. For broader application thresholds need to be applied to account for variations, but it may serve as a practical tool for determining when more detailed investigations are warranted. However, precise evaluations using these metrics inherently depend on the specific characteristics of each system and therefore require individualized assessment.

5.2 Ethical Considerations

As engineers, it is important to recognize the potential ethical and societal impacts of our work. Although initially, very few aspects of this thesis were thought to have such influence, it became increasingly evident over the course of this work that different screening metrics can significantly affect the future integration of renewable energy sources. Therefore, it is crucial to thoroughly understand all facets and implications of the metrics used to ensure that a stable power system is maintained while continuing to reduce the carbon footprint of electricity generation.

One risk associated with screening metrics is the unforeseen exploitation of loopholes by individual market operators. This issue has already been demonstrated in Australia by AEMO with their experience of using AFL for screening new connections. Since AFL utilizes the MSCR of CBRs, a high MSCR indicates that a large portion of the available short circuit power will be absorbed by the converter. Market participants realized that there was little incentive to minimize their own MSCR values. As a result, some participants reported inflated MSCR figures with the intent to slow down the approval processes for other CBR projects. These inflated MSCR values increased the likelihood of additional time-consuming EMT studies for competitors.

From the perspective of the Swedish TSO, the risk of similar exploitation is mitigated by impocing project-specific requirements on new large CBR connections. In the later stages of such a process, developers are required to conduct comprehensive impedance based stability studies and submit detailed EMT models. This enables the Swedish TSO to verify the performance characteristics of any newly connected CBRs and maintain an accurate understanding of system conditions. As a result, the influence of previously connected CBRs can be properly accounted for and the risk of individual tampering is reduced.

5.3 Future Work and Research

Based on the findings of this thesis, several areas warrant further research. One particular area of interest is the continued evaluation of EqSCR across varying types

of CBRs. This thesis focused primarily on wind farms, but many other CBRs are present in the power system. All CBRs exhibit different tolerances to system strength and oscillations depending on their control characteristics, but in particular HVDC devices are of great interest, as their rated capacities can be several times greater than those of other individual CBRs in the network, which may disproportionately affect interaction and stability. The increasing deployment of battery energy storage systems, PV generation and STATCOMs also raises questions about their impact on system strength metrics like EqSCR.

Another area of interest is the role of loads in system strength assessment. The network models used in this thesis were dominated by generation resources. Future studies could investigate systems with more balanced generation-to-load ratios, or scenarios with high load levels, to determine how load affects system strength. Additionally, the impact of large converter-based loads, such as data centers and hydrogen electrolyzers, on system strength requires careful consideration, especially given the numerous planned projects of this type in northern Sweden.

An additional topic for research is the weighting of CBR interactions within EqSCR using MIIF. The current approach assumes that all interactions contribute linearly. However, since a low interaction factor indicates minimal risk, it is worth exploring whether contributions from CBRs with low MIIF should be penalized or disregarded. This refinement could improve the accuracy of EqSCR and ensure it does not provide an overly conservative estimation of system strength.

Finally, another aspect that is likely to become increasingly important is the impact of Grid-Forming (GFM) converters. This thesis has focused exclusively on system strength and stability related to Grid-Following (GFL) converters, as they currently represent the predominant type in the power system. However, GFM converter technology is rapidly advancing, and future European grid codes may even require the adoption of GFM converters, given that these devices exhibit certain beneficial characteristics compared to GFL converters [37]. Understanding the influence of increasing penetration of GFM converters is essential for ensuring accurate system strength estimation as power systems evolve in the future.

6
Conclusion

This thesis has investigated the evolving challenges associated with power system strength assessment arising from the increasing penetration of CBRs. The initial evaluation of traditional SCR was consistent with findings reported in previous studies, highlighting the well-documented limitations of SCR in accurately capturing stability issues in systems with multiple closely located CBRs, as well as its inherent restriction to phenomena occurring at the nominal 50 Hz frequency. This limitation becomes especially evident when comparing SCR-based assessments to the impedance-based analysis, as demonstrated in Section 4.1.1, which show that SCR only reflects system behavior at 50 Hz, while impedance based stability analysis can provide a more detailed evaluation across a larger frequency spectrum.

Since the thesis investigats system strength screening aimed at early-stage grid planning, the study of alternative metrics focuses on understanding SCR-based metrics and associated interaction factors. While interaction factors can be difficult to apply in isolation to assess system strength, they are used within SCR-based metrics, justifying their inclusion in the analysis. Evaluation through small-scale case studies identified AFL, EqSCR, and SDSCR as the most promising alternatives. These metrics were subsequently implemented as PSS®E scripts for further evaluation.

The evaluation of SCR, AFL, EqSCR, and SDSCR in PSCAD demonstrated that the traditional SCR tends to overestimate system strength under conditions of high penetration of CBRs, with values ranging from 4.2 to 4.5 for Cases A–C, despite the presence of instability. When the amount of CBRs was reduced, the SCR estimate improved marginally but still displayed a tendency toward overestimation. AFL exhibited inconsistent performance; for Cases A–C, it produced positive values even in unstable conditions, indicating overestimated system strength. However, its accuracy improved when the share of CBRs was lower, with AFL returning negative values under unstable conditions, as expected.

EqSCR and SDSCR yielded more reliable and consistent results. Both metrics successfully identified weak system conditions, with instability observed in Type 3 wind turbines when connected at EqSCR values below approximately 1.1–1.3 and SDSCR values below 1.15–1.4. Nevertheless, due to its lower computational complexity, EqSCR was considered more suitable for large scale screening of system strength in the initial planning of a converter-dominated power systems.

Based on these findings, this thesis recommends the use of EqSCR for system

strength assessment under high levels of CBR penetration. The commonly used thresholds for screening with EqSCR are found to be largely appropriate. While the classification of a very weak system for EqSCR<2 is considered accurate, a slight adjustment is proposed for the threshold of EqSCR=3 used to distinguish between weak and strong system strength. Instead, an updated threshold of EqSCR=2.5 is recommended. Although these thresholds may appear conservative, given that instability was not observed until EqSCR dropped below 1.3, they provide a necessary margin to account for variations in network configuration. Different topologies, control parameters, and converter characteristics can significantly influence stability as a result of phenomena not exhibited at 50 Hz, and which are therefore not adequately captured by SCR-based metrics. This is, however, a trade-off that has to be made between accuracy and complexity for screening metrics to be useful in early planning of the power system.

One aspect of this thesis that could benefit from further research is the impact of other CBR types on EqSCR, as this project has only focused on two types of converter-based wind farms in simulations. Of particular interest are large-scale solar PV and HVDC systems. Solar PV converters often exhibit less robust control behavior, potentially requiring increased system strength for stable operation. HVDC systems, due to their higher rated power, may have a disproportionate impact on system interactions. Another critical area for future investigation is the role of emerging GFM converters. This thesis has focused exclusively on GFL converters, which currently dominate the system. However, as GFM technology continues to grow, it is essential to understand how its characteristics affect system strength estimation and stability.

References

[1] UN, *The paris agreement*, Accessed: 2025-05-05. [Online]. Available: https://www.un.org/en/climatechange/paris-agreement.

[2] IEA, *Renewables 2023*, Accessed: 2025-01-30, 2024. [Online]. Available: https://www.iea.org/reports/renewables-2023.

[3] SCB, *Installerad generatoreffekt, mw efter elområde, kraftslag och år*, Accessed: 2025-01-29, 2025. [Online]. Available: https://www.statistikdatabasen.scb.se/pxweb/sv/ssd/START__EN__EN0105__EN0105A/AnlInstEffBrProd/table/tableViewLayout1/.

[4] S. Chakraborty, M. G. Simoes, and W. E. Kramer, Eds., *Power Electronics for Renewable and Distributed Energy Systems*. London: Springer, 2013. DOI: 978-1-4614-1109-2.

[5] F. Blaabjerg and K. Ma, "Wind energy systems," *Proceedings of the IEEE*, vol. 105, no. 11, pp. 2116–2131, 2017. DOI: 10.1109/JPROC.2017.2695485.

[6] Energinet, Fingrid, Statnett, and Svenska Kraftnät. "Nordic grid development perspective 2023." Accessed: Mar. 27, 2025. (2023), [Online]. Available: https://www.svk.se/siteassets/om-oss/rapporter/2023/svk_ngpd2023.pdf.

[7] E. Nycander, T. Jakobsson, and E. Hellström. "Långsiktig marknadsanalys, Scenarier för kraftsystemets utveckling fram till 2050." Accessed: Jul. 10, 2025. (2024), [Online]. Available: https://www.svk.se/siteassets/om-oss/rapporter/2024/lma_2024.pdf.

[8] B. Badrzadehand, M. V. Escudero, Y. Liao, and Y. Zhu, "Screening methods as preliminary calculations to determine the level and type of dynamic modeling required," in *Power System Dynamic Modelling and Analysis in Evolving Networks*, B. Badrzadehand and Z. Emin, Eds. Springer, 2024, ch. 5, ISBN: 978-3-031-47821-5.

[9] F. Blaabjerg and K. Ma, "Wind energy systems," *Proceedings of the IEEE*, vol. 105, no. 11, pp. 2116–2131, 2017. DOI: 10.1109/JPROC.2017.2695485.

[10] CIGRE WG B4.62, "Connection of wind farms to weak ac networks," Cigre, Tech 671, 2016. [Online]. Available: https://www.e-cigre.org/publications/detail/671-connection-of-wind-farms-to-weak-ac-networks.html.

[11] P. Kundur *et al.*, "Definition and classification of power system stability," *IEEE Transactions on Power Systems*, vol. 19, no. 3, pp. 1387–1401, 2004. DOI: 10.1109/TPWRS.2004.825981.

[12] N. Hatziargyriou *et al.*, "Definition and classification of power system stability – revisited & extended," *IEEE Transactions on Power Systems*, vol. 36, no. 4, 2021. DOI: 10.1109/TPWRS.2020.3041774.

[13] M. Lindner *et al.*, "Suitable classification of power system stability phenomena," in *Proceedings of CIGRÉ Symposium 2025 in Trondheim*, 2025.

[14] H. H. Alhelou, N. Hosseinzadeh, and B. Bahrani, *Power System Strength - Evaluation Methods, Best Practice, Case Studies, and Applications*. Institution of Engineering and Technology (The IET), 2024, ISBN: 978-1-83953-807-0. [Online]. Available: https://app.knovel.com/hotlink/toc/id:kpPSSEMBP1/power-system-strength/power-system-strength.

[15] "Integrating inverter-based resources into low short circuit strength systems, Reliability guidleine," NERC, 3353 Peachtree Road NE, Suite 600 North Tower Atlanta, 2017. [Online]. Available: https://www.nerc.com/comm/RSTC_Reliability_Guidelines/Item_4a._Integrating%20_Inverter-Based_Resources_into_Low_Short_Circuit_Strength_Systems_-_2017-11-08-FINAL.pdf.

[16] A. Boričić, J. L. R. Torres, and M. Popov, "System strength: Classification, evaluation methods, and emerging challenges in ibr-dominated grids," in *2022 IEEE PES Innovative Smart Grid Technologies - Asia (ISGT Asia)*, 2022, pp. 185–189. DOI: 10.1109/ISGTAsia54193.2022.10003499.

[17] L. Liyanarachchi, N. Hosseinzadeh, A. Gargoom, and E. M. Farahani, "A new index for the assessment of power system strength considering reactive power injection and interaction of inverter based resources," *Sustainable Energy Technologies and Assessments*, vol. 60, 2023. DOI: https://doi.org/10.1016/j.seta.2023.103460.

[18] W. Chao, S. Subham, and B. Frede, "Robust synchronization for high penetration of inverter based resources," *IEEE Smart Grid Bulletin*, Jun. 2021, Accessed: 2025-06-15. [Online]. Available: https://smartgrid.ieee.org/bulletins/june-2021/robust-synchronization-for-high-penetration-of-inverter-based-resources.

[19] Y. Guo, "Impedance analysis of three-phase lcl-type grid- connected inverters with adaptive pll," in *2019 3rd International Conference on Electronic Information Technology and Computer Engineering (EITCE)*, 2019, pp. 21–27. DOI: 10.1109/EITCE47263.2019.9094906.

[20] R. Rogersten, F. Hohn, and O. Lennerhag, "Managing stability in the future converter-dominated swedish power system," in *Proceedings of the CIGRÉ Session 2025*, 2025.

[21] J. Sun, "Frequency-domain stability criteria for converter-based power systems," *IEEE Open Journal of Power Electronics*, vol. 3, pp. 222–254, 2022. DOI: 10.1109/OJPEL.2022.3155568.

[22] Y. Zhang, S.-H. F. Huang, J. Schmall, J. Conto, J. Billo, and E. Rehman, "Evaluating system strength for large-scale wind plant integration," in *2014 IEEE PES General Meeting | Conference & Exposition*, 2014. DOI: 10.1109/PESGM.2014.6939043.

[23] J. Matevosyan. "Wecc workshop – weak grid experiences in ercot." Presentation. (2021), [Online]. Available: https://www.esig.energy/download/wecc-workshop-weak-grid-experiences-in-ercot-julia-matevosyan/.

[24] "Essential reliability services task force measures framework report," NERC, 3353 Peachtree Road NE, Suite 600 North Tower Atlanta, 2015. [Online]. Available: https://www.nerc.com/pa/RAPA/ra/Reliability%20Assessments%20DL/ERSTF%20Framework%20Report%20-%20Final.pdf.

[25] D. Wu, G. Li, M. Javadi, A. M. Malyscheff, M. Hong, and J. N. Jiang, "Assessing impact of renewable energy integration on system strength using site-dependent short circuit ratio," *IEEE Transactions on Sustainable Energy*, vol. 9, no. 3, pp. 1072–1080, 2018. DOI: 10.1109/TSTE.2017.2764871.

[26] CIGRE WG 14.07 and IEEE WG 15.05.05, "Guide for planning dc links terminating at ac locations having low short-circuit capacities, Part 1: Ac/dc interaction phenomena," Cigre, IEEE, Technical brochure 068, 1992. [Online]. Available: https://www.e-cigre.org/publications/detail/068-guide-for-planning-dc-links-terminating-at-ac-locations-having-low-short-circuit-capacities-part-1-acdc-interaction-phenomena.html.

[27] A. Ekic, B. Strombeck, D. Wu, and G. Ji, "Assessment of grid strength considering interactions between inverter-based resources and shunt capacitors," in *2020 IEEE Power & Energy Society General Meeting (PESGM)*, 2020, pp. 1–5. DOI: 10.1109/PESGM41954.2020.9281633.

[28] CIGRE WG B4.41, "Systems with multiple dc infeed," Cigre, Technical brochure 364, 2008. [Online]. Available: https://www.e-cigre.org/publications/detail/364-systems-with-multiple-dc-infeed.html.

[29] D. Kim and B. Lee, "Impact of renewable energy sources on ac system strength using inverter interaction level," in *2019 IEEE Sustainable Power and Energy Conference (iSPEC)*, 2019, pp. 1217–1221. DOI: 10.1109/iSPEC48194.2019.8975093.

[30] CIGRE WG C4.56, "Electromagnetic transient simulation models for large-scale system impact studies in power systems having a high penetration of inverter-connected generation," Cigre, Technical brochure 881, 2022. [Online]. Available: %5Curl%7Bhttps://www.e-cigre.org/publications/detail/881-electromagnetic-transient-simulation-models-for-large-scale-system-impact-studies-in-power-systems-having-a-high-penetration-of-inverter-connected-generation.html%7D.

[31] CIGRE Joint Work Group C4/B4.52, "Guidelines for subsynchronous oscillation studies in power electronics dominated power systems," Cigre, Technical brochure 909, 2023. [Online]. Available: https://www.e-cigre.org/publications/detail/909-guidelines-for-subsynchronous-oscillation-studies-in-power-electronics-dominated-power-systems.html.

[32] M. Annakkage, C. Karawita, and U. Annakkage, "Frequency scan-based screening method for device dependent sub-synchronous oscillations," in *2016 IEEE Power and Energy Society General Meeting (PESGM)*, 2016. DOI: 10.1109/PESGM.2016.7741623.

[33] N.a, *Typ4 4 wind turbine model*, Revision 3, Accessed: 2025-02-28, Manitoba Hydro International, 2018. [Online]. Available: %5Curl%7Bhttps://www.google.com/url?sa=t&rct=j&q=&esrc=s&source=web&cd=&ved=2ahUKEwjvtLCEieaLAxWuUVUIHYZ3MCQQFnoECAwQ%20AQ&url=https%3A%2F%2Fwww.pscad.com%2Fuploads%2Fknowledge_base%2Ftype_4_wind_turbine_model_v46.pdf%3Ft%3D1544110359&usg=AOvVaw1lhn0vkDChYOuo%20mBmYqG3I&opi=89978449%7D.

[34] N.a, *Type 3 wind turbine model*, Revision 3, Accessed: 2025-02-10, Manitoba Hydro International, 2018. [Online]. Available: %5Curl%7Bhttps://www.google.com/url?sa=t&rct=j&q=&esrc=s&source=web&cd=&ved=2ahUKEwjh3bWDkJuMAxXXgSoKHVJzLVUQFnoECBAQAQ&url=https%3A%2F%2Fwww.pscad.com%2Fuploads%2Fknowledge_base%2Ftype_3_wind_turbine_model_v45.pdf&usg=AOvVaw0CFlxTxiVIUt5dwCkLIDfk&opi=89978449%7D.

[35] C. Zhang, X. Wang, F. Blaabjerg, W. Wang, and C. Liu, "The influence of phase-locked loop on the stability of single-phase grid-connected inverter," in *2015 IEEE Energy Conversion Congress and Exposition (ECCE)*, 2015, pp. 4737–4744. DOI: 10.1109/ECCE.2015.7310329.

[36] Fingrid, *Utilizing equivalent short-circuit ratio (escr) approach for assessing the slow converter driven stability and tuning the voltage controllers*, Accessed: 2025-06-04, 2023. [Online]. Available: https://www.fingrid.fi/globalassets/dokumentit/fi/palvelut/kulutuksen-ja-tuotannon-liittaminenkantaverkkoon/white-paper-on-escr.pdf.

[37] Agency for the Cooperation of Energy Regulators, *Nc rfg dc recommendation: Annex 1 - amended rfg regulation*, Available: https://www.acer.europa.eu/sites/default/files/documents/Recommendations_annex/ACER_Recommendation_03-2023_Annex_1_NC_RfG_clean.pdf, 2023.

A

PSSE Base Model: Data

This appendix presents the parameters for the base model introduced in section 3.3.1, since no standardized model such as the IEEE 37 bus system was used. This appendix includes data for machine, two winding transformer, branches and fixed shunts. To allow for the case studies performed in section 4.3.2 to be replicated. The base power of this system is 1000 MVA

Table A.1: Machine data for PSS®E model

Bus	Mbase [MVA]	Pgen [MW]	Pmax [MW]	Qgen [Mvar]	Qmax [Mvar]
1	1000.0	-1459.4	9999.0	256.5	9999.0
5	1000.0	389.9	9999.0	-91.8	9999.0
18	100.0	80.0	100.0	23.6	25.0
19	85.0	80.0	85.0	16.7	55.0
20	85.0	80.0	85.0	16.7	55.0
23	100.0	75.0	100.0	3.6	48.75
24	100.0	80.0	100.0	15.5	65.0
25	100.0	80.0	100.0	15.6	65.0
26	85.0	80.0	85.0	3.8	30.0
27	100.0	100.0	100.0	19.6	35.0
28	100.0	95.0	100.0	17.2	30.0
29	100.0	95.0	100.0	19.4	30.0
30	100.0	95.0	100.0	20.9	30.0
33	100.0	95.0	100.0	24.9	65.0
34	75.0	70.0	75.0	7.9	48.75
35	75.0	70.0	75.0	7.9	48.75
36	75.0	70.0	75.0	10.4	24.0
37	75.0	70.0	75.0	10.9	24.0

Table A.2: Two winding transformer data for PSS®E model

Bus 1	Bus 2	Wind. 1 [kV]	Wind. 2 [kV]	Winding MVA [MVA]	R [pu]	X [pu]
4	6	420.0	140.0	500.0	0.001	0.15
4	7	420.0	140.0	500.0	0.001	0.15
8	18	140.0	33.0	120.0	0.003	0.12
9	19	140.0	33.0	100.0	0.003	0.12
9	20	140.0	33.0	100.0	0.003	0.12
10	23	140.0	33.0	120.0	0.003	0.12
11	24	140.0	33.0	120.0	0.003	0.12
11	25	140.0	33.0	120.0	0.003	0.12
12	26	140.0	33.0	100.0	0.003	0.12
13	27	140.0	33.0	120.0	0.003	0.12
13	28	140.0	33.0	120.0	0.003	0.12
14	29	140.0	33.0	120.0	0.003	0.12
14	30	140.0	33.0	120.0	0.003	0.12
15	33	140.0	33.0	110.0	0.003	0.12
15	31	140.0	33.0	120.0	0.003	0.12
15	32	140.0	33.0	120.0	0.003	0.12
16	34	140.0	33.0	80.0	0.003	0.12
16	35	140.0	33.0	80.0	0.003	0.12
17	36	140.0	33.0	80.0	0.003	0.12
17	37	140.0	33.0	80.0	0.003	0.12
58	59	420.0	140.0	500.0	0.001	0.15

Table A.3: Shunt data for base model in PSS®E

Bus	B-shunt [MVAr]	Bus	B-shunt [MVAr]
6	50	27	3.0
7	50	28	5.0
18	1.5	29	3.5
19	2.0	30	2.0
20	2.0	33	1.0
23	2.0	34	1.0
24	1.5	35	1.0
25	1.5	36	1.5
		37	1.0

Table A.4: Branch data for base model in PSS®E

From bus	To bus	RX [pu]	Line charging B [pu]
1	4	(0.01+0.15j)	0.07
2	3	-0.15j	0.0
2	58	(0.005+0.075j)	0.035
3	4	(0.01+0.15j)	0.07
5	58	(0.005+0.075j)	0.035
6	7	0.0001j	0.0
6	9	(0.03+0.32j)	0.0016
6	13	(0.03+0.32j)	0.0016
7	14	(0.0225+0.24j)	0.0012
7	15	(0.06+0.64j)	0.0032
8	59	(0.045+0.48j)	0.0024
10	11	(0.0195+0.208j)	0.001
10	59	(0.0525+0.56j)	0.0028
12	13	(0.0315+0.336j)	0.0017
13	14	(0.015+0.16j)	0.0008
14	16	(0.027+0.288j)	0.0014
15	16	(0.018+0.192j)	0.00096
16	17	(0.027+0.288j)	0.0014

B

Scripts for Alternative System Strength Metrics

The scripts developed for automated calculation of AFL, EqSCR and SDSCR could only be included for the internal version of the report for SVK due to the use of some internally developed functions and the possible future use of the scripts developed in this project.

B.1 Script AFL

B.2 Script EqSCR

B.3 Script SDSCR

C

Extended Results Section 4.3.2

This appendix presents the detailed results for the simulations performed for section 4.2.1. It presents the alternative metrics calculated using the developed scripts for all CBR-buses for the respective case in PSS®E.

Table C.1: Results calculation system strength for variations of Case A

		Case A				Case A x 1.1				Case A x 1.2				Case A x 1.3			
Bus	SC_i	SCR	AFL	EqSCR	SDSCR	SCR	AFL	EqSCR	SDSCR	SCR	AFL	EqSCR	SDSCR	SCR	AFL	EqSCR	SDSCR
18	530	6.6	271	2.75	2.79	6.0	246	2.5	2.54	5.5	221	2.29	2.32	5.1	196	2.08	2.15
19	553	6.9	351	2.06	2.12	6.3	333	1.87	1.93	5.8	315	1.71	1.77	5.3	297	1.55	1.63
20	553	6.9	351	2.06	2.12	6.3	333	1.87	1.93	5.8	315	1.71	1.77	5.3	297	1.55	1.63
23	508	6.8	293	2.22	2.27	6.2	274	2.02	2.06	5.6	255	1.85	1.89	5.2	236	1.66	1.74
24	462	5.8	237	2.05	2.1	5.2	217	1.87	1.9	4.8	196	1.7	1.75	4.4	176	1.54	1.61
25	462	5.8	237	2.05	2.1	5.2	217	1.87	1.91	4.8	196	1.7	1.75	4.4	176	1.54	1.61
26	500	6.2	213	1.8	1.86	5.7	187	1.63	1.69	5.2	161	1.49	1.55	4.8	135	1.35	1.43
27	682	6.8	298	1.9	1.96	6.2	263	1.72	1.78	5.7	230	1.58	1.64	5.2	196	1.44	1.51
28	680	7.2	310	1.91	1.98	6.5	278	1.74	1.8	6.0	246	1.59	1.65	5.5	214	1.45	1.52
29	694	7.3	322	1.92	1.98	6.6	290	1.74	1.8	6.1	258	1.59	1.65	5.6	226	1.45	1.53
30	695	7.3	324	1.92	1.98	6.7	291	1.74	1.8	6.1	259	1.59	1.65	5.6	227	1.45	1.53
33	590	6.2	330	1.78	1.86	5.6	308	1.62	1.69	5.2	286	1.48	1.55	4.8	264	1.35	1.43
34	481	6.9	287	1.71	1.79	6.2	270	1.56	1.62	5.7	254	1.42	1.49	5.3	238	1.29	1.38
35	481	6.9	287	1.71	1.79	6.2	270	1.56	1.62	5.7	254	1.42	1.49	5.3	238	1.29	1.38
36	425	6.1	165	1.6	1.67	5.5	141	1.45	1.52	5.1	118	1.33	1.39	4.7	95	1.2	1.29
37	425	6.1	165	1.6	1.67	5.5	142	1.45	1.52	5.1	118	1.33	1.4	4.7	95	1.2	1.29
		Stable				Stable				Stable				Unstable			

Table C.2: Results calculation system strength for variations of Case B

		Case B				Case B x 1.1				Case B x 1.2			
Bus	SC_i	SCR	AFL	EqSCR	SDSCR	SCR	AFL	EqSCR	SDSCR	SCR	AFL	EqSCR	SDSCR
18	440	5.5	150.0	1.45	1.49	5.0	123.0	1.32	1.36	4.6	97.0	1.21	1.24
19	507	6.3	276.0	1.4	1.45	5.8	257.0	1.27	1.32	5.3	238.0	1.16	1.21
20	507	6.3	276.0	1.4	1.45	5.8	257.0	1.27	1.32	5.3	238.0	1.16	1.21
23	424	5.7	173.0	1.28	1.33	5.1	152.0	1.16	1.21	4.7	132.0	1.06	1.11
24	392	4.9	135.0	1.22	1.27	4.5	112.0	1.11	1.15	4.1	91.0	1.01	1.06
25	392	4.9	135.0	1.22	1.27	4.5	112.0	1.11	1.15	4.1	91.0	1.01	1.06
26	460	5.8	147.0	1.26	1.32	5.2	120.0	1.14	1.2	4.8	94.0	1.04	1.1
27	613	6.1	184.0	1.32	1.38	5.6	148.0	1.2	1.25	5.1	113.0	1.09	1.15
28	611	6.4	197.0	1.33	1.38	5.8	163.0	1.2	1.26	5.4	129.0	1.1	1.15
29	623	6.6	205.0	1.33	1.39	6.0	170.0	1.21	1.26	5.5	137.0	1.1	1.16
30	624	6.6	206.0	1.33	1.39	6.0	172.0	1.21	1.26	5.5	138.0	1.1	1.16
33	537	5.7	242.0	1.26	1.33	5.1	219.0	1.15	1.21	4.7	196.0	1.05	1.11
34	445	6.4	226.0	1.22	1.29	5.8	208.0	1.11	1.17	5.3	192.0	1.01	1.08
35	445	6.4	226.0	1.22	1.29	5.8	208.0	1.11	1.17	5.3	192.0	1.01	1.08
36	397	5.7	116.0	1.16	1.23	5.2	92.0	1.06	1.12	4.7	68.0	0.96	1.03
37	397	5.7	117.0	1.16	1.23	5.2	92.0	1.06	1.12	4.7	69.0	0.96	1.03
		Stable				Unstable				Unstable			

Table C.3: Results calculation system strength for variations of Case C

		Case C				Case C x 1.1				Case C x 1.2				Case C x 1.3			
Bus	SC_i	SCR	AFL	EqSCR	SDSCR	SCR	AFL	EqSCR	SDSCR	SCR	AFL	EqSCR	SDSCR	SCR	AFL	EqSCR	SDSCR
18	530	6.6	271.0	2.75	2.79	6.0	246.0	2.5	2.54	5.5	221.0	2.29	2.33	5.1	196.0	2.12	2.15
19	510	6.4	306.0	2.16	2.2	5.8	288.0	1.96	2.0	5.3	270.0	1.79	1.83	4.9	251.0	1.66	1.69
20	510	6.4	306.0	2.16	2.2	5.8	288.0	1.96	2.0	5.3	270.0	1.79	1.83	4.9	251.0	1.66	1.69
23	508	6.8	293.0	2.22	2.27	6.2	274.0	2.02	2.06	5.6	255.0	1.84	1.89	5.2	236.0	1.71	1.74
24	462	5.8	237.0	2.05	2.1	5.2	217.0	1.86	1.91	4.8	196.0	1.7	1.75	4.4	176.0	1.58	1.61
25	462	5.8	237.0	2.05	2.1	5.2	217.0	1.86	1.91	4.8	196.0	1.7	1.75	4.4	176.0	1.58	1.61
26	433	5.4	144.0	1.87	1.92	4.9	117.0	1.7	1.75	4.5	91.0	1.55	1.6	4.2	64.0	1.44	1.48
27	567	5.7	188.0	1.98	2.02	5.2	153.0	1.8	1.84	4.7	119.0	1.64	1.69	4.4	85.0	1.52	1.56
28	565	5.9	201.0	2.0	2.04	5.4	167.0	1.81	1.86	5.0	135.0	1.66	1.7	4.6	102.0	1.54	1.57
29	606	6.4	231.0	1.84	1.92	5.8	198.0	1.67	1.75	5.3	165.0	1.53	1.6	4.9	133.0	1.41	1.48
30	607	6.4	232.0	1.84	1.93	5.8	199.0	1.67	1.75	5.3	166.0	1.53	1.61	4.9	134.0	1.42	1.48
33	535	5.6	264.0	1.72	1.81	5.1	241.0	1.56	1.64	4.7	218.0	1.42	1.51	4.3	195.0	1.32	1.39
34	441	6.3	236.0	1.65	1.74	5.7	219.0	1.5	1.58	5.2	202.0	1.37	1.45	4.8	185.0	1.26	1.34
35	441	6.3	236.0	1.65	1.74	5.7	219.0	1.5	1.58	5.2	202.0	1.37	1.45	4.8	185.0	1.26	1.34
36	394	5.6	124.0	1.55	1.63	5.1	100.0	1.4	1.48	4.7	76.0	1.28	1.36	4.3	52.0	1.18	1.26
37	394	5.6	124.0	1.55	1.63	5.1	100.0	1.4	1.48	4.7	76.0	1.28	1.36	4.3	52.0	1.18	1.26
		Stable				Stable				Stable				Unstable			

Table C.4: Results calculation system strength for variations of Case D

		Case D				Case D x 1.4				Case D x 1.8				Case D x 2.0			
Bus	SC_i	SCR	AFL	EqSCR	SDSCR	SCR	AFL	EqSCR	SDSCR	SCR	AFL	EqSCR	SDSCR	SCR	AFL	EqSCR	SDSCR
18	530	6.6	276.0	3.51	3.57	4.7	177.0	2.51	2.55	3.7	78.0	1.95	1.99	3.3	29.0	1.75	1.79
19	553	6.9	371.0	3.05	3.14	4.9	303.0	2.18	2.25	3.8	236.0	1.7	1.75	3.5	203.0	1.53	1.57
23	508	6.8	319.0	3.06	3.12	4.8	248.0	2.18	2.23	3.8	179.0	1.7	1.73	3.4	146.0	1.53	1.56
24	462	5.8	271.0	2.87	2.93	4.1	198.0	2.05	2.09	3.2	127.0	1.59	1.63	2.9	91.0	1.43	1.47
26	500	6.2	229.0	2.59	2.68	4.5	127.0	1.85	1.91	3.5	27.0	1.44	1.49	3.1	-30.0	1.27	1.32
27	682	6.8	329.0	2.78	2.87	4.9	198.0	1.98	2.05	3.8	70.0	1.54	1.6	3.4	6.0	1.38	1.44
29	694	7.3	355.0	2.84	2.93	5.2	230.0	2.02	2.09	4.1	108.0	1.57	1.63	3.7	47.0	1.41	1.47
33	590	6.2	354.0	2.6	2.69	4.4	269.0	1.85	1.93	3.5	186.0	1.44	1.5	3.1	145.0	1.29	1.35
34	481	6.9	306.0	2.54	2.64	4.9	243.0	1.81	1.89	3.8	181.0	1.41	1.47	3.4	151.0	1.26	1.32
36	425	6.1	189.0	2.42	2.51	4.3	100.0	1.72	1.79	3.4	12.0	1.33	1.4	3.0	-32.0	1.2	1.26
		Stable				Stable				Stable				Unstable			

Table C.5: Results calculation system strength for variations of Case E

		Case E				Case E x 1.4				Case E x 1.8				Case E x 2.2			
Bus	SC_i	SCR	AFL	EqSCR	SDSCR	SCR	AFL	EqSCR	SDSCR	SCR	AFL	EqSCR	SDSCR	SCR	AFL	EqSCR	SDSCR
18	530	6.6	281.0	4.15	4.23	4.7	183.0	2.96	3.02	3.7	85.0	2.31	2.35	3.0	-12.0	1.89	1.92
19	553	6.9	374.0	3.4	3.5	4.9	306.0	2.43	2.5	3.8	239.0	1.89	1.95	3.1	173.0	1.54	1.6
23	508	6.8	348.0	4.16	4.24	4.8	286.0	2.97	3.03	3.8	224.0	2.31	2.36	3.1	162.0	1.9	1.93
27	682	6.8	343.0	3.2	3.3	4.9	214.0	2.28	2.36	3.8	88.0	1.77	1.83	3.1	-37.0	1.45	1.5
29	694	7.3	364.0	3.21	3.31	5.2	240.0	2.29	2.37	4.1	119.0	1.78	1.84	3.3	-1.0	1.45	1.51
33	590	6.2	359.0	2.88	2.98	4.4	274.0	2.05	2.13	3.5	191.0	1.59	1.66	2.8	110.0	1.3	1.36
34	481	6.9	309.0	2.83	2.93	4.9	246.0	2.01	2.09	3.8	185.0	1.56	1.63	3.1	125.0	1.27	1.33
36	425	6.1	192.0	2.67	2.77	4.3	103.0	1.9	1.98	3.4	15.0	1.48	1.54	2.8	-73.0	1.2	1.26
		Stable				Stable				Stable				Unstable			

Table C.6: Results calculation system strength for variations of Case F

		Case F				Case F x 1.8				Case F x 2.2				Case F x 2.8			
Bus	SC_i	SCR	AFL	EqSCR	SDSCR	SCR	AFL	EqSCR	SDSCR	SCR	AFL	EqSCR	SDSCR	SCR	AFL	EqSCR	SDSCR
19	553	6.9	381.0	4.44	4.57	3.8	248.0	2.47	2.54	3.1	182.0	1.99	2.08	2.5	84.0	1.58	1.64
29	694	7.3	384.0	4.41	4.54	4.1	146.0	2.45	2.53	3.3	28.0	1.99	2.07	2.6	-148.0	1.57	1.63
33	590	6.2	374.0	3.87	4.0	3.5	211.0	2.15	2.22	2.8	132.0	1.74	1.82	2.2	13.0	1.38	1.44
36	425	6.1	201.0	3.6	3.71	3.4	27.0	1.99	2.06	2.8	-59.0	1.62	1.69	2.2	-188.0	1.27	1.33
		Stable				Stable				Stable				Unstable			

DEPARTMENT OF SOME SUBJECT OR TECHNOLOGY
CHALMERS UNIVERSITY OF TECHNOLOGY
Gothenburg, Sweden
www.chalmers.se

CHALMERS
UNIVERSITY OF TECHNOLOGY